OPEN ACCESS
Freely Available Online

OpenAccessPub

Journal of New Developments in Chemistry
ISSN NO: 2377-2549

Research Article

DOI : 10.14302/issn.2377-2549.jndc-17-1488

Molecular Structure and Vibrational Analysis Of 2-(4-Methoxyphenyl)-2, 3-Dihydro-1H-Perimidine Using Density Functional Theory

A. Nathiya[a], H. Saleem[a]*, T.Jayakumarb, A.Rajavel[b], N. Ramesh Babu[c]

[a]Department of Physics, Annamalai University, Annamalainagar 608 002, Tamil Nadu, India
[b]Department of Chemistry (FEAT), Annamalai University, Annamalainagar 608 002, Tamil Nadu, India
[c]Department of Physics, M.I.E.T. Engineering College, Tiruchirappalli – 620 007, Tamil Nadu, India
*Corresponding author

Abstract:

The compound 2-(4-methoxyphenyl)-2, 3-dihydro-1H-perimidine (MPDP) was synthesized. The molecular structure and its functional groups were characterized with the help of Fourier Transform Infrared: FTIR/ Fourier Transform FT-Raman spectra in the regions of 400-4000/50-4000cm^{-1}, respectively. The geometrical parameters, harmonic vibrational wavenumbers, Infrared (IR) & Raman scattering intensities, Nuclear Magnetic Resonance (NMR) chemical shift and Ultraviolet-Visible (UV-Vis) spectra were computed using B3LYP/6-311++G(d,p) level of theory. The complete vibrational analysis were made on the basis of Potential energy distribution (PED) calculation with the help of VEDA4 programme. The Highest occupied molecular orbital (HOMO) – Lowest unoccupied molecular orbital (LUMO) energy gap and intra-molecular charge transfer (ICT) were studied using NBO analysis. The first order hyperpolarizability (β_0) and other related properties (β, α_0, $\Delta\alpha$) of MPDP were computed. The molecular electrostatic potential (MEP), Mulliken atomic charges were calculated using the same level of theory. In addition, the various thermodynamic parameters were also calculated.

Corresponding author :

H. Saleem, Department of Physics, Annamalai University, Annamalainagar 608 002, Tamil Nadu, India.
E-mail: saleem_h2001@yahoo.com

Citation: A.Nathiya , H.Saleem , T.Jayakumar , A.Rajavel , N.Ramesh Babu (2017) Molecular Structure and Vibrational Analysis of 2-(4-methoxyphenyl)-2, 3-Dihydro-1H-Perimidine using Density Functional Theory. Journal of New Developments in Chemistry - 1(2):70-99. https://doi.org/10.14302/issn.2377-2549.jndc-17-1488

Keywords: FT-IR; FT-Raman, UV, NMR; PED; NBO; MPDP, HOMO-LUMO; MEP; MK, Docking.
Received : Mar 18, 2017 **Accepted :** Apr 08, 2017 **Published:** Apr 20, 2017
Academic Editor: Zhe-Sheng Chenz, Professor Department of Pharmaceutical Sciences College of Pharmacy and Allied Health Professions St. John's University

Introduction

Perimidine derived schiff base have been extensively studied in recent years owing to their great variety of biological activity such as, anti-malarial, antibacterial, anti-tumoral, antiviral activities, etc. [1–6]. Higher π acidity and the presence of more than one hetero atom in pyrimidine play an important role in its co -ordination chemistry, compared to that of pyridine bases, and serve as better models in biological systems [7–9]. Because of perimidine group of organic molecules are reported at scarce. Usually the heterocyclic compounds are used to drug designing in the organic system and the great importance due to possible promising in medical applications [10–16]. Such compounds undergo oxidative aromatization and hydrolysis of the dihydropyrimidine ring. Preparative methods have been developed to facilitate the selective oxidative aromatization or hydrolytic elimination of the dihydropyrimidine fragment of the compounds [17]. This kind of compound have been attractive for physicochemical applications of non-linear optical [18], electrical property [19], chelating agents in metal–ligand chemistry as fluorescent liquid crystals [20]. Dihydropyrimidinones, the product of the Biginelli reaction, are also widely used in the pharmaceutical industry as calcium channel blockers and alpha-1 antagonists [21]. Moreover, some bioactive alkaloids such as batzelladine B, containing the dihydropyrimidine unit, which has been isolated from marine sources, show anti-HIV activity [22].

The biologically relevant molecule 2-(thiophen-2-yl)-2,3-dihydro-1H-perimidine was synthesized and characterized by FT-IR, UV, NMR, MS, CHN microanalysis and X-ray crystallography as well as by DFT/B3LYP/6-311++G(d,p) calculations. The vibrational bands observed in the FTIR spectrum were assigned. The molecular properties like HOMO-LUMO analysis, MEP mapping, chemical reactivity descriptors, dipole moment and natural charges were calculated using the same level of basis set. The results of molecular docking admitted that perimidine may exhibit enzyme inhibitor activity.

In the present study, MPDP molecule was synthesized and characterized by FT-IR, FT-Raman NMR and UV-Vis spectroscopy techniques. The structural and vibrational behavior of the MPDP molecule were carried out using the quantum chemical calculation with the help of DFT/B3LYP/6-311++G (d,p) level of theory.

Experimental details

Synthesis

The compound MPDP was synthesized by refluxing 4-methoxy benzaldehyde 0.05mol) with 1, 8-diaminonaphthalene 0.05mol) in methanol solution 60ml) for 4 hour. The resulting solution was evaporated in air by slow evaporation to remove the solvent. The product was collected by filtration, washed several time with methanol and recrystallized from hot methanol. The recrystallized product was dried in desiccators under vaccum over anhydrous $CaCl_2$.

FT-IR, FT-Raman, NMR and UV-Vis spectra details

The FT-IR spectrum in the spectral range 4000-400 cm^{-1} was recorded using KBr pellet technique with a FT-IR-Shimadzu spectrometer. The spectrum was recorded at room temperature with a scanning speed of 10 cm^{-1} per minute at the spectral resolution of 2.0 cm^{-1} on Instrumentation laboratory, Jamal Mohamed College, Tiruchirappalli, Tamilnadu. FT-Raman spectrum was observed using laser source Nd: YAG 1064 nm as excitation wavelength in the region 50-4000 cm^{-1} on Bruker IFS 66v spectrophotometer equipped with a FRA 106 FT-Raman module accessory at the spectral resolution of 4 cm^{-1}. The FT-Raman spectrum was recorded at SAIF Laboratory, IIT Madras. The UV-Vis absorption spectrum of MPDP was recorded in the range of 200-500 nm using a Perkin Elmer Lambda-35 spectrometer. The UV pattern was taken from a 10^{-5} molar solution of MPDP dissolved in methanol, recorded at ACIC, St. Joseph's College, Tiruchirapalli, Tamilnadu. ^{1}H

NMR spectra were recorded on a Bruker 400 MHz spectrometer spectrum is recorded on a Bruker 100 MHz spectrometer in the department of chemistry, Annamalai University, Annamalai Nagar. Chemical shift values are reported in parts per million (ppm) and tetramethylsilane (TMS) as internal standard.

Computational methods

The entire calculations were performed at DFT levels on a Pentium IV/3.02 GHz personal computer using Gaussian 03W [25] program package, invoking gradient geometry optimization [25, 26]. In this study, the density functional three parameter hybrid model DFT/B3LYP/6-311++G (d,p) basis set was used to calculated various properties of the title molecule. The vibrational modes were assigned on the basis of TED analysis with the help of VEDA4 program [27] and by combining results of Gauss View program [28] with symmetry considerations. It should be noted that the Gaussian 03W package is unable to calculate the Raman activity. The Raman activities were transformed into Raman intensities using Raint program [29] by the expression:

$$I_i = 10^{-12} \times (\nu_0 - \nu_i)^4 \times \frac{1}{\nu i} \times RA_i \qquad (1)$$

Where I_i is the Raman intensity, Ai is the Raman scattering activities, m_i is the wavenumber of the normal modes and m_0 denotes the wavenumber of the excitation laser [30].

Molecular docking study:

Molecular docking experiment was carried out to study the exact binding location of ligand on protein. Molecular docking simulation was performed with the Argus Lab 4.0. The prepared 3D structures of 1JIJ protein was downloaded from the protein data bank (see http://www.rcsb.org/pdb) and binding site was made by choosing "Making binding site for this protein" option. The ligand was then introduced and docking calculation was allowed to run using shape-based search algorithm and A Score scoring function. The scoring function is responsible for evaluating the energy between the ligand and protein target. Flexible docking was allowed by constructing grids over the binding sites of the protein and energy based rotation is set for that ligand group of atoms that do not have rotatable bonds. For each rotation, torsions are created and poses (conformation) are generated during the docking process. For each complex 10 independent runs were conducted and one pose was returned for each run. The best docking model was selected according to the lowest binding energy calculated by Argus lab and the most suitable binding conformation was selected on the basis of hydrogen bond interaction between the ligand and protein near the substrate binding site. The lowest energy poses indicate the highest binding affinity as high energy produces the unstable conformations. The resulting receptor model was saved to Brookhaven PDB file from the file the 2D and 3D interactions are viewed in discovery studio 4.5 versions.

Result and discussion

NMR analysis

NMR spectroscopy is a useful technique to establish the structure and nature of the compound. The ^1H NMR spectrum of the compound MPDP was recorded in $CDCl_3$ using tetramethyl silane (TMS) as internal standard. ^1H NMR spectrum of the compound showed a sharp singlet peak at δ6.839ppm corresponding to C-H proton. A doublet observed at δ9.01ppm with integral value 2 is attributed to >N-H proton in perimidine ring. The multiple signals observed between δ7.196 and 7.836ppm are related to aromatic protons. A sharp peak appeared at δ2.197ppm with an integral value three confirm the presence of $-OCH_3$ group in the compound. Thus ^1H NMR results confirmed the formation of MPDP by the condensation of 1, 8, diaminonapthalene and 4-methoxy benzaldehyde. The observed NMR spectral value is listed in Table 1 and the

^{1}H NMR spectrum is shown in Fig 1.

Molecular geometry

Table 1. The ^{1}H NMR Analysis of MPDP

Compounds	^{1}H NMR functional groups with chemical shift in δ, ppm)			
	-OCH3	-NH	Aromatic Proton	-HC
Ligand	2.197	4.011, 4.025	7.194-7.836	6.839

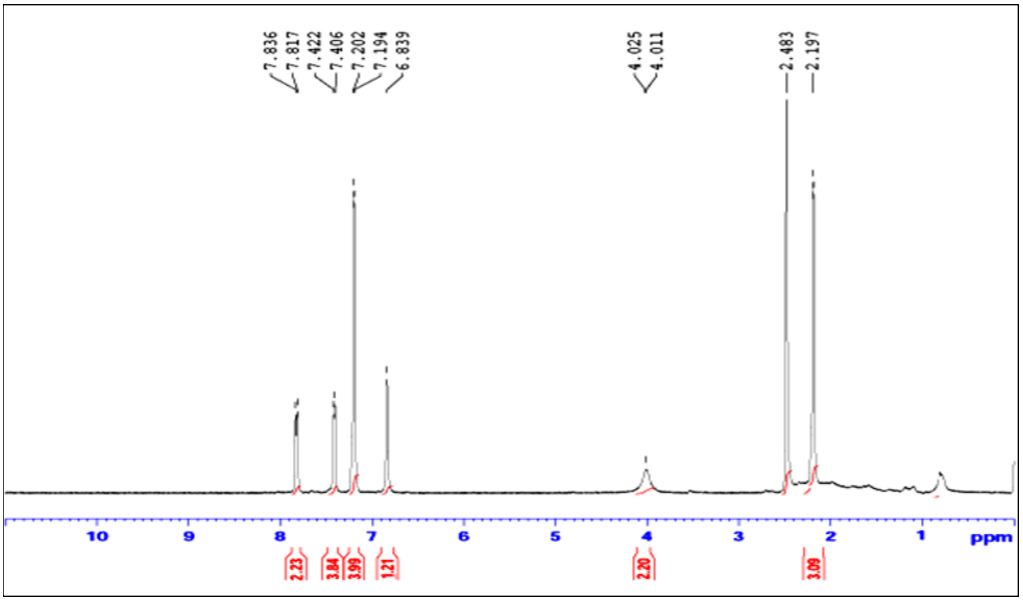

Fig.1. The ^{1}H NMR spectrum

The optimized molecular structure of MPDP molecule with atom numbering scheme is shown in Fig.2. The geometrical parameters (Bond lengths, bond angles and dihedral angles) of the title compound was calculated by DFT method and are listed in Table 2. To the best of our knowledge there is no exact crystal data is available for this compound and therefore we have compared the bond parameters with the crystal data of the related molecule.

It is evident from the Table 2, that the deviations are observed in case of C-H, and N-H bond length while other bond length are in agreement with the literature [23]. The calculated C-H bond length of perimidine ring (except:C21-H22) is deviated slightly (~ 0.1547Å) from the literature value [23], which may be arise from the low, scattering factors of hydrogen atoms in the x-ray diffraction [23]. Normally the C-H bond distance is observed around 1.0840Å, whereas the calculated bond length of C21-H22 is 1.063Å. This negative (~ 0.02 Å) deviation is due to the existence of twisted boat configuration caused by the methoxy substitution at C21 atom. The bond C21-C23 has lesser bond length (1.5112Å) among the other C-C bonds. These may be due to the attachment of methoxyphenyl with C21 atom.

In perimidine ring, the various bond angles are found to be consistent with literature value [23]. The bond angles of C_5-C_4-C_9/C_2-C_3-C_8 are calculated as 122.83°/119. 91°, respectively and are differ by 2.92°. This observation confirmed the involvement of C_2-C_3-C_8 carbon chain in of perimidine ring structure. The calculated bond angles $C_{25}C_{28}H_{32}$/$C_{24}C_{26}H_3$ and $C_{30}C_{28}H_{32}$/ $C_{30}C_{26}H_{31}$ are found at 121.35°/119.28° and 118.73°/121.04°, respectively. Furthermore, the bond angles $C_{28}C_{30}O_{33}$ (115.87°) and $C_{26}C_{30}O_{33}$ (124.48°) are differ by (~ 8.61°). These observations suggest the distortion of the bulky methoxy group.

The dihedral angle of C3-C2-N17-C21 is 29.26

Table 2. The optimized bond parameters of MPDP using B3LYP/6-311++G(d,p) level

Parameters Bond lengths (Å)	B3LYP/ 6-311++G(d,p)	XRD
C1-C2	1.3842	1.366
C1-C6	1.4097	1.386
C1-H7	1.0852	0. 930
C2-C3	1.4267	1.414
C2-N17	1.3968	1.392
C3-C4	1.4265	1.412
C3-C8	1.4267	1.417
C4-C5	1.4197	1.401
C4-C9	1.4197	1.401
C5-C6	1.3764	1.353
C5-H10	1.0841	0. 930
C6-H11	1.0847	0. 930
C8-C13	1.3842	0. 930
C8-N18	1.3968	1.389
C9-C12	1.3764	1.345
C9-H14	1.0841	0. 930
C12-C13	1.4097	1.398
C12-H15	1.0847	0. 930
C13-H16	1.0852	0. 930
N17-H19	1.011	0.85
N17-C21	1.4642	1.439
N18-H20	1.011	0.830
N18-C21	1.4642	1.461
C21-H22	1.1063	0. 980
C21-C23	1.5112	
C23-C24	1.3953	
C23-C25	1.3988	
C24-C26	1.3937	
C24-H27	1.0836	
C25-C28	1.3883	
C25-H29	1.0855	
C26-C30	1.3998	
C26-H31	1.0817	
C28-C30	1.3993	
C28-H32	1.0832	
C30-O33	1.363	
O33-C34	1.4222	
C34-H35	1.0952	
C34-H36	1.0886	
C34-H37	1.0952	

Table 2 continued from page 10

Bond Angles (°)		
C2-C1-C6	120.0186	119.7
C2-C1-H7	119.9307	120.2
C6-C1-H7	120.0504	120.2
C1-C2-C3	119.7025	120.1
C1-C2-N17	122.7373	122.7
C3-C2-N17	117.5132	117.1
C2-C3-C4	120.0261	119.6
C2-C3-C8	119.9053	120.2
C4-C3-C8	120.0261	120.2
C3-C4-C5	118.5802	118.2
C3-C4-C9	118.5801	117.7
C5-C4-C9	122.8328	124.0
C4-C5-C6	120.2589	120.8
C4-C5-H10	119.1122	119.6
C6-C5-H10	120.6271	119.6
C1-C6-C5	121.4094	121.6
C1-C6-H11	118.7938	119.2
C5-C6-H11	119.7963	119.2
C3-C8-C13	119.7026	119.3
C3-C8-N18	117.5127	117.4
C13-C8-N18	122.7376	123.2
C4-C9-C12	120.2591	121.5
C4-C9-H14	119.112	119.3
C12-C9-H14	120.6271	119.3
C9-C12-C13	121.4094	120. 9
C9-C12-H15	119.7964	119.5
C13-C12-H15	118.7938	119.5
C8-C13-C12	120.0185	120.4
C8-C13-H16	119.9309	119.8
C12-C13-H16	120.0503	119.8
C2-N17-H19	114.7908	
C2-N17-C21	116.5255	118.3
H21-N17-C19	113.1188	112.0
C8-N18-H20	114.791	113.0
C8-N18-C21	116.5251	116.5
C21-N18-H20	113.1181	113.0
N17-C21-N18	106.5097	106.9
N17-C21-H22	109.6684	109.7
N17-C21-C23	111.24	
N18-C21-H22	109.6678	109.7
N18-C21-C23	111.2394	
H22-C21-C23	108.4973	
C21-C23-C24	120.7247	
C21-C23-C25	120.7357	
C24-C23-C25	118.5396	
C23-C24-C26	121.132	
C23-C24-H27	119.1549	
C26-C24-H27	119.7131	
C23-C25-C28	121.0692	
C23-C25-H29	119.6509	
C28-C25-H29	119.28	
C24-C26-C30	119.6825	
C24-C26-H31	119.2783	
C30-C26-H31	121.0392	
C25-C28-C30	119.9275	
C25-C28-H32	121.348	
C30-C28-H32	118.7246	
C26-C30-C28	119.6493	
C26-C30-O33	124.481	
C28-C30-O33	115.8697	
C30-O33-C34	118.7307	
O33-C34-H35	111.4097	
O33-C34-H36	105.7893	
O33-C34-H37	111.4094	
H35-C34-H36	109.3197	
H35-C34-H37	109.501	
H36-C34-H37	109.3201	

Table 2 continued from page 11

Dihedral Angles (°)		
C6-C1-C2-C3	0.111	
C6-C1-C2-N17	-177.3328	-176.7
H7-C1-C2-C3	179.9167	
H7-C1-C2-N17	2.4729	-2.7
C2-C1-C6-C5	-0.1427	-0.5
C2-C1-C6-H11	-179.9052	
H7-C1-C6-C5	-179.9482	-179.8
H7-C1-C6-H11	0.2893	-0.128
C1-C2-C3-C4	-0.4098	
C1-C2-C3-C8	-178.0381	
N17-C2-C3-C4	177.166	177.0
N17-C2-C3-C8	-0.4624	2.4
C1-C2-N17-H19	-17.688	18.5
C1-C2-N17-C21	-153.2424	155.7
C3-C2-N17-H19	164.8155	164.0
C3-C2-N17-C21	29.2611	26.8
C2-C3-C4-C5	0.7224	0.5003
C2-C3-C4-C9	-178.3484	
C8-C3-C4-C5	178.3478	
C8-C3-C4-C9	-0.7229	
C2-C3-C8-C13	178.0387	-179.8
C2-C3-C8-N18	0.4635	2.4
C4-C3-C8-C13	0.4104	-0.30
C4-C3-C8-N18	-177.1648	
C3-C4-C5-C6	-0.7531	-0.0028
C3-C4-C5-H10	179.7372	-179. 9
C9-C4-C5-C6	178.2757	-179.6
C9-C4-C5-H10	-1.234	-0.304
C3-C4-C9-C12	0.7534	0.003
C3-C4-C9-H14	-179.7371	-179. 9
C5-C4-C9-C12	-178.2755	179.6
C5-C4-C9-H14	1.2341	-0.304
C4-C5-C6-C1	0.4711	-0.20
C4-C5-C6-H11	-179.7688	179.8
H10-C5-C6-C1	179.9732	179.8
H10-C5-C6-H11	-0.2666	0.12
C3-C8-C13-C12	-0.1114	0.58
C3-C8-C13-H16	-179.9167	-179.89
N18-C8-C13-C12	177.3319	-176.7
N18-C8-C13-H16	-2.4735	2.7
C3-C8-N18-H20	-164.816	-164.0
C3-C8-N18-C21	-29.263	-26.8
C13-C8-N18-H20	17.6879	-18.5
C13-C8-N18-C21	153.241	-155.7
C4-C9-C12-C13	-0.471	0.20
C4-C9-C12-H15	179.769	179.8
H14-C9-C12-C13	-179.9731	-179.8
H14-C9-C12-H15	0.2669	
C9-C12-C13-C8	0.1427	
C9-C12-C13-H16	179.9478	179. 9

Table 2 continued from page 12

Dihedral Angles (°)		
H15-C12-C13-C8	179.905	179.8
H15-C12-C13-H16	-0.2898	0.26
C2-N17-C21-N18	-54.1289	47.1
C2-N17-C21-H22	64.4735	
C2-N17-C21-C23	-175.5003	
H19-N17-C21-N18	169.5971	-175.0
H19-N17-C21-H22	-71.8004	
H19-N17-C21-C23	48.2258	
C8-N18-C21-N17	54.13	
C8-N18-C21-H22	-64.4728	
C8-N18-C21-C23	175.5018	
H20-N18-C21-N17	-169.597	
H20-N18-C21-H22	71.8002	
H20-N18-C21-C23	-48.2252	
N17-C21-C23-C24	59.278	
N17-C21-C23-C25	-120.7225	
N18-C21-C23-C24	-59.2881	
N18-C21-C23-C25	120.7114	
H22-C21-C23-C24	179.9955	
H22-C21-C23-C25	-0.005	
C21-C23-C24-C26	179.9994	
C21-C23-C24-H27	-0.0003	
C25-C23-C24-C26	-0.0001	
C25-C23-C24-H27	-179.9999	
C21-C23-C25-C28	-179.9987	
C21-C23-C25-H29	0.0009	
C24-C23-C25-C28	0.0008	
C24-C23-C25-H29	180.0005	
C23-C24-C26-C30	-0.0007	
C23-C24-C26-H31	179.9992	
H27-C24-C26-C30	179.9991	
H27-C24-C26-H31	-0.0011	
C23-C25-C28-C30	-0.0007	
C23-C25-C28-H32	179.9997	
H29-C25-C28-C30	179.9997	
H29-C25-C28-H32	0.0001	
C24-C26-C30-C28	0.0008	
C24-C26-C30-O33	-180.0004	
H31-C26-C30-C28	180.001	
H31-C26-C30-O33	-0.0003	
C25-C28-C30-C26	-0.0002	
C25-C28-C30-O33	180.001	
H32-C28-C30-C26	-180.0006	
H32-C28-C30-O33	0.0006	
C26-C30-O33-C34	-0.0008	
C28-C30-O33-C34	-180.002	
C30-O33-C34-H35	61.3032	
C30-O33-C34-H36	179.9994	
C30-O33-C34-H37	-61.304	

and C3-C8-N18-C21 is -29.26. This dihedral angle indicated that N17-C21-N18 ring portion projected in the upward direction to attain the twisted boat configuration. This twisted boat configuration is attained due to the steric effect of methoxy group substituted at C_{21} atom.

Vibrational assignments

The MPDP molecule pocess C_1 point group symmetry. It consists of 37 atoms, and hence 105 normal modes of vibrations are possible and are also distributed as: 71 in-plane bending and 34 out-of-plane bending vibrations. The detailed vibrational assignment are made on the basis of PED analysis using VEDA4 program [31]. The calculated frequencies are usually higher than the corresponding experimental quantities, due to the combination of electron correlation effects and basis set deficiencies. These discrepancies were overcome by applying the appropriate scaling factors; the theoretical calculations reproduce the experimental data well in agreement. The calculated wavenumbers scaled with a proper scale factor [32]. The simulated and observed FT-IR and FT-Raman spectra are shown in Figs. 3 and 4, respectively. The experimental and scaled theoretical harmonic vibrational frequencies along with the calculated PED values are given in Table. 3.

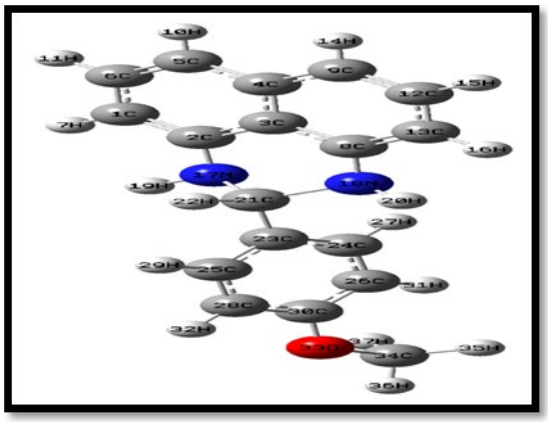

Fig-2. Optimized structure of 2-(4-methoxyphenyl)-2, 3-dihydro-1H perimidine (MPDP)

N-H vibrations

Zhuomin Li et al., [33] assigned the ν_{NH}, β_{NH} and Γ_{NH} at 3367, 1278 and 544cm^{-1}, respectively in the case of 1′,3′-dihydrospiro [fluorene-9,2′-perimidine]. The stretching and in-plane bending modes of NH group of perimidine ring in 2-(thiophene-2yl)-2,3-dihydro-1H-perimidine (TDP) were respectively assigned at 3413 and 1516cm^{-1} in FTIR spectrum [23]. The IR absorption bands due to ν_{NH} mode usually occur in the region of 3200-3500cm^{-1} [34]. The β_{NH} vibration is an important mode, which shows their presence as medium to strong bands in the region 1549-1520cm^{-1} [34].

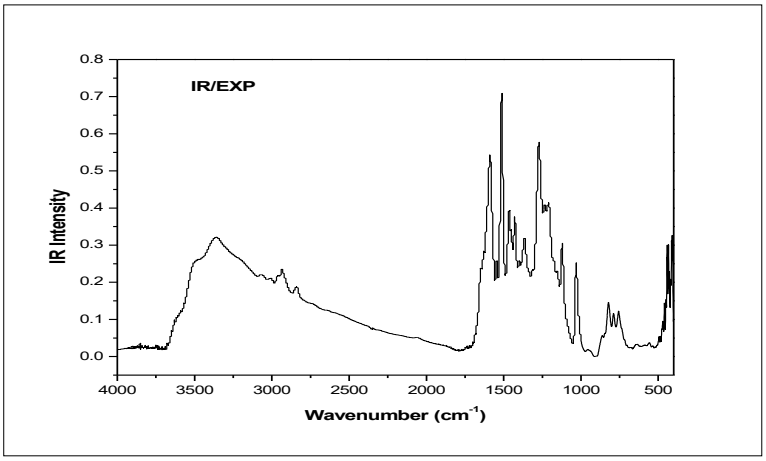

Fig. 3. Combined experimental and theoretical FT-IR spectra of MPDP

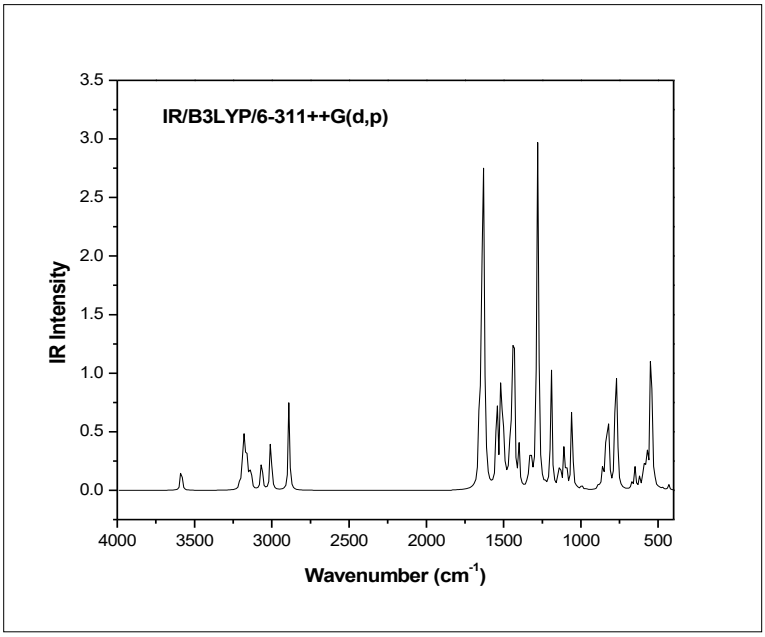

Fig. 4. Combined experimental and theoretical FT-Raman spectra of MPDP

Table. 3. The experimental and calculated frequencies of MPDP using B3LYP/6-311++G(d,p) level of basis set [harmonic frequencies (cm^{-1}), IR, Raman intensities (Km/mol), reduced masses (amu) and force constants ($mdynA°^{-1}$)]

Mode No.	Calculated Frequencies (cm^{-1})		Observed Frequencies (cm^{-1})		IR Intensity	Raman Intensity	Reduced Masses	Force Consts.	Vibrational Assignments≥10% (PED)[d]
	Un Scaled	Scaled[a]	FT-IR	FT-Raman	Rel.[b]	Rel.[c]			
1	3586	3445			6.85	0.44	1.08	8.15	vN17H19(100)
2	3586	3445	3357 w	3244 w	4.56	2.15	1.08	8.16	vN17H19(100)
3	3207	3081	3076 w	3080 w	3.06	1.75	1.09	6.62	vC26H31(99)
4	3194	3068			2.19	2.75	1.09	6.57	vC28H32(93)
5	3186	3061			2.11	0.48	1.09	6.51	vC24H27(99)
6	3184	3059			11.89	8.14	1.10	6.55	vC1H7(98)
7	3182	3057			12.36	1.18	1.10	6.54	vC1H7(99)
8	3168	3044		3043 w	4.64	3.37	1.09	6.44	vC5H10(98)
9	3167	3043			6.50	0.02	1.09	6.44	vC1H7(99)
10	3161	3037			4.09	0.92	1.09	6.41	vC25H29(94)
11	3156	3032			8.66	0.18	1.09	6.37	vC1H7(98)
12	3156	3032			0.05	1.97	1.09	6.37	vC1H7(99)
13	3136	3013	3013 w		10.68	2.79	1.10	6.37	vC34H36(91)
14	3066	2946	2934 w		15.64	1.02	1.11	6.13	vC34H35(99)
15	3007	2889	2839 w		25.69	3.45	1.03	5.51	vC34H37(91)
16	2889	2776			35.44	2.00	1.08	5.32	vC21H22(100)
17	1660	1595			18.65	0.29	6.14	9.96	βH7C1C2(46)+vC1C2(23)
18	1651	1586	1589 m	1591 m	18.20	3.93	5.83	9.37	vC21N18(74)+βH27C24C26(19)
19	1634	1570			188.95	14.61	5.80	9.12	vC12C13(55)
20	1626	1562			17.72	11.46	5.95	9.26	vC1C6(76)+βH10C5C4(18)
21	1617	1554	1544 w		19.53	1.32	6.55	10.09	vC23C24(68)+βC24C26C30(26)
22	1549	1489	1512 s		0.01	0.13	3.80	5.37	vC1C6(49)+vC1C2(26)+βH7C1C2(20)+vC1C6(24)
23	1544	1484			47.62	0.94	2.55	3.58	βH27C24C26(23)+vC21C23(20)+vC26C30(32)
24	1517	1457	1464 m		52.21	11.23	1.68	2.28	βH10C5C4(58)
25	1504	1445			24.61	1.22	1.06	1.42	βH35C34H37(68)+τH35C34O33C30(25)
26	1493	1435			4.12	1.29	1.05	1.37	βH35C34H36(66)+ΓC34H35O33H36(26)
27	1492	1433	1428 w		1.26	0.71	2.69	3.53	vC1C2(36)+βH7C1C2(33)
28	1476	1418			3.07	0.34	1.19	1.53	βH35C34H36(81)
29	1468	1410			0.50	0.07	1.64	2.09	βH19N17C2(52)+τH22C21C23C24(32)

Table 3 continued from page 15

Mode No.	Calculated Frequencies (cm^{-1})		Observed Frequencies (cm^{-1})		IR Intensity	Raman Intensity	Reduced Masses	Force Consts.	Vibrational Assignments≥10% (PED)[d]
	Un Scaled	Scaled[a]	FT-IR	FT-Raman	Rel.[b]	Rel.[c]			
30	1461	1404			12.21	2.07	2.16	2.71	νC24C26(33)+βH7C1C2(21)+βH32C28C30(20) +βH10C5C4(25)
31	1447	1391			17.46	1.38	2.21	2.73	νC12C13(38)+βH10C5C4(55)
32	1435	1379	1365 w	1374 w	100.00	2.40	3.74	4.53	νC24C26(23)+νC1C2(33)
33	1401	1346			15.73	13.79	5.07	5.86	νC2C3(33)+νC3C4(24)
34	1385	1331			0.46	3.96	2.08	2.35	νC2C3(18)+βH7C1C2(40)
35	1349	1296			1.19	0.05	2.39	2.56	βH7C1C2(25)+νC1C2(28)+τH22C21C23C24(32)
36	1333	1280		1280 w	10.80	1.25	2.85	2.98	νC23C24(21)+βH7C1C2(46)
37	1322	1271	1271 s		6.85	2.50	1.81	1.86	νC23C24(20)+βH7C1C2(56)
38	1316	1265			4.99	0.71	1.23	1.26	βH19N17C2(12)+τH22C21C23C24(42)
39	1285	1235			52.56	6.63	1.57	1.52	νC12C13(38)+βH7C1C2(51)
40	1278	1228			127.37	2.41	4.21	4.05	νO33C30(59)
41	1268	1219	1212 m		6.75	1.24	2.84	2.69	τH22C21C23C24(32)+νN17C2(15)+νC4C5(33) +νC1C6(24)
42	1234	1185		1190 w	0.10	0.16	1.87	1.68	νC1C2(36)+βH7C1C2(53)
43	1229	1181			0.95	11.48	2.30	2.05	βH27C24C26(15)+νC21C23(70)
44	1207	1159			0.05	0.08	1.28	1.10	νC1C6(26)+βH10C5C4(68)
45	1201	1154			5.52	0.86	1.42	1.21	βH35C34H37(38)+τH35C34O33C30(45)
46	1190	1144			40.16	2.62	1.17	0.98	νC23C24(24)+βH27C24C26(29)+νC26C30(32)
47	1190	1143			4.21	0.29	1.37	1.14	νC1C2(18)+βH7C1C2(51)
48	1168	1122			0.27	0.34	1.27	1.02	βH35C34H36(16)+ΓC34H35O33H36(46)
49	1147	1102			4.12	1.18	1.92	1.49	νC1C6(25)+βH7C1C2(36)
50	1136	1092			8.02	0.63	3.96	3.01	νC1C6(74)
51	1133	1088			3.10	0.05	1.31	0.99	νC24C26(23)+βH32C28C30(61)
52	1109	1065		1077 w	15.40	1.57	1.95	1.41	βH10C5C4(25)+νC1C2(63)
53	1094	1051			10.03	6.42	2.39	1.69	νC1C6(29)+νN17C21(56)
54	1058	1017	1030 m		30.98	0.76	6.72	4.43	νO33C34(72)+νC26C30(12)
55	1054	1012			3.72	0.28	3.43	2.24	νC4C5(40)+βC3C2N17(18)
56	1026	986			1.11	0.10	2.63	1.63	βH27C24C26(43)+τH19N17C2C1(14)
57	995	956			2.29	1.59	4.41	2.57	νN18C21(76)
58	976	938			0.04	0.02	1.34	0.75	τH27C24C26C30(34)+τC8C13C9C12(41)
59	973	935			0.24	0.24	1.29	0.72	τH7C1C2N17(38)+βC8C13C12(34)
60	967	929			0.01	0.01	1.29	0.71	τH7C1C2N17(61)
61	960	922			0.12	0.00	1.35	0.73	τH27C24C26C30(17)+ΓC21C23C25C24(33)
62	886	851	863 w		2.20	2.74	3.95	1.83	νN18C8(53)
63	875	840			0.34	0.49	1.55	0.70	τH7C1C2N17(51)
64	861	827			7.06	0.01	3.00	1.31	βC4C9C12(28)+τH27C24C26C30(32)+βC3C2N17 (18)

www.openaccesspub.org | JNDC CC-license DOI : 10.14302/issn.2377-2549.jndc-17-1488 Vol-1 Issue –2 Page No- 80

OPEN ACCESS Freely Available Online

OpenAccessPub

Table 3 continued from page 16

Mode No.	Calculated Frequencies (cm^{-1})		Observed Frequencies (cm^{-1})		IR Intensity	Raman Intensity	Reduced Masses	Force Consts.	Vibrational Assignments≥10% (PED)[d]
	Un Scaled	Scaled[a]	FT-IR	FT-Raman	Rel.[b]	Rel.[c]			
65	855	821	822 w		0.12	0.22	1.43	0.62	τH7C1C2N17(52)
66	842	809			15.26	0.03	2.07	0.86	βC4C9C12(28)+τH27C24C26C30(22)+βC21C23C25(27)
67	826	794		797 w	25.76	0.86	4.08	1.64	τH7C1C2N17(21)+τC8C13C9C12(35)+βC28C30O33(26)
68	825	793			1.79	0.05	1.29	0.52	τH27C24C26C30(61)
69	818	786	789 w		13.52	3.67	4.56	1.80	νC1C2(53)+βC2C1C6(28)
70	792	761	756 w		0.13	3.25	4.64	1.71	νO33C30(59)+νC26C30(22)
71	776	745			42.78	0.31	5.16	1.83	βC2C1C6(38)+βN17C21N18(32)
72	767	737			34.36	0.02	1.57	0.54	τH7C1C2N17(21)+βC28C30O33(46)
73	755	725			0.03	0.13	1.31	0.44	τH7C1C2N17(22)+ τH10C5C4C9(70)
74	744	715	701 w		0.36	0.54	3.67	1.20	τH27C24C26C30(27)+τC8C13C9C12(30)
75	671	645	639 w		2.39	12.72	5.04	1.34	νN18C8(33)+νC2C3(44)
76	651	626			0.23	0.08	3.05	0.76	ΓC1C3N17C2(29)
77	650	624			8.14	1.28	5.48	1.36	βC24C26C30(26)+τC8C13C9C12(45)
78	641	616			0.17	1.47	4.81	1.17	βC24C26C30(16)+τC8C13C9C12(25)+βC28C30O33(16) +ΓC8C2C4C3(22)
79	620	596			4.13	0.28	2.68	0.61	βC4C9C12(18)+ΓC8C2C4C3(15)+τC9C4C12C13(25)+βC3C2N17 (18)
80	594	570			11.71	0.45	2.30	0.48	βC23C21N18(21)+τH27C24C26C30(22)+τC9C4C12C13(25) +τC8C13C9C12(30)
81	574	551	558 w		17.35	8.87	5.88	1.14	νC2C3(44)+βC8N18C21(36)
82	546	524			85.88	3.72	1.35	0.24	ΓC5C3C9C4(61)
83	532	511			0.45	0.48	2.85	0.48	τC9C4C12C13(25)+τH19N17C2C1(16)+ΓO33C26C28C30(27) +βC21C23C25(17)
84	521	501			1.88	2.74	4.93	0.79	βC3C2N17(18)+βC8N18C21(36)
85	507	487	494 w		0.12	1.07	3.55	0.54	τH19N17C2C1(26)+τC25C28C26C30(30)+ΓO33C26C28C30(27)
86	495	476			0.75	0.60	4.76	0.69	τH19N17C2C1(36)+βC21C23C25(47)
87	473	455	459 w		0.83	0.04	3.44	0.45	βC8C13C12(44)+ΓC8C2C4C3(32)
88	464	446	448 m		0.18	0.59	4.87	0.62	ΓC1C3N17C2(45)
89	432	415			2.18	0.70	4.35	0.48	νN18C8(23)+νN17C21(16)+νC1C2(13)+βN17C21N18(22)
90	429	413			0.01	0.60	3.09	0.34	τH27C24C26C30(24)+τC8C13C9C12(31)
91	416	399			0.05	6.56	3.16	0.32	τC9C4C12C13(35)+ΓC1C3N17C2(52)
92	361	347			0.16	0.20	5.45	0.42	βC26C30C28(57)
93	323	310			1.34	3.23	3.98	0.25	βC24C26C30(42)+βC28C30O33(39)
94	261	251			2.42	0.79	3.72	0.15	βC24C26C30(72)
95	257	247			0.00	0.40	3.47	0.13	τC25C28C26C30(67)
96	238	228			0.21	0.68	1.27	0.04	βC3C2N17(14)
97	230	221			1.15	2.89	6.41	0.20	νC1C2(33)+βC24C26C30(42)
98	172	166			3.05	1.51	4.40	0.08	τC6C1C2N17(49)
99	170	164			0.39	0.77	3.11	0.05	βC23C21N18(21)+βC21C23C25(27)+τC6C1C2N17(10) +τC2N17N18C21(13)
100	144	138			0.43	3.90	4.55	0.06	βC28C30O33(19)+τC23C25C30C28(29)+ΓC8C2C4C3(22)
101	142	136			0.23	0.81	4.29	0.05	τC2N17N18C21(58)
102	95	91			1.52	2.40	3.59	0.02	βC23C21N18(31)+βC26C30C28(27)+τC6C1C2N17(10)
103	42	41			0.05	31.32	5.17	0.01	βC28C30O33(19)+τC23C25C30C28(29)+τH35C34O33C30(31)
104	40	38			0.10	19.16	4.59	0.00	βC23C21N18(61)+τC2N17N18C21(33)
105	29	27			0.31	100.00	3.70	0.00	ΓC1C3N17C2(57)

In the present molecule the observed vibrational frequencies at 3357/3244 cm^{-1} in FT-IR/ FT-Raman spectra and its corresponding calculated values are at 3445/3445 cm^{-1}(mode no: 1& 2) are assigned to vN–H mode. These modes are in expected regions and also find support from PED value (100%). The observed frequencies are negatively (~ 88cm^{-1}) deviated from harmonic frequencies, which is due to the presence of moderate unharmonicity in this vibration as well as may be the participation of NH bond in the inter-molecular hydrogen-bonding interactions occur with in the molecule/crystal [23]. The N–H in-plane bending modes ($\beta H_{19}N_{17}C_2$ are assigned at 1410 and 1265cm^{-1} in MPDP molecule (mode nos: 29 & 38). The N-H torsional mode $\tau H_{19}N_{17}C_2C_1$ is assigned at 494 cm^{-1} in FT-IR spectrum and for the same mode the corresponding harmonic values are 487, 476cm^{-1} (mode nos:85, 86) harmonic values. The above assignments are consistent with literature [23] and also find support from PED values 52, 12 and 26, 36%).

C-H vibrations:

The bands vibrating at 2935, 2851cm^{-1} in FTIR spectrum were ascribed to C-H stretching vibrations of perimidine ring in TDP by M. Alum et al., [23]. The scaled harmonic frequencies in the range 3059-3032cm^{-1} (mode nos:6-9, 11, 12) are attributed to ν_{C-H} modes of perimidine ring MPDP. It should be mentioned here that these ν_{C-H} modes are pure and having >98% of PED value.

In aromatic compounds, the ν_{C-H}, β_{C-H} and Γ_{C-H} bending modes appear in the ranges of 3100-3000, 1300-1000 and 1000-750cm^{-1}, respectively [35]. In this study, there are eleven C-H stretching βC-H and ΓC-H vibrations are possible for MPDP]. As revealed by PED, the phenyl ring ν_{C-H} modes are undoubtedly assigned at 3081, 3068, 3061 and 3037cm^{-1} (mode nos: 3-5, 10). The observed weak bands at 3076/3080cm^{-1} (FTIR/FT-Raman) are in agreement with mode no: 3. The theoretically calculated values of C-H in-plane bending vibrations of phenyl ring vibrations fall in the region 1404-986cm^{-1} (mode nos:30, 46, 51, 56). Similarly the harmonic bands due to C-H out-of-plane bending vibration fall in the region 938-715cm^{-1} (mode nos:58, 64, 68, 74). In this study, the experimental bands are missing for β_{CH} mode, which may be due to the steric factor of bulky group (naphthalene ring). The β_{CH} and τ_{CH} modes are within the expected region with few exceptions and also having considerable PED values: >20 and 27%, respectively. The observed FTIR band at 701cm^{-1} is further support the mode no:74. Literature survey reveal that the CH group shows characteristic frequency band due to stretching/in-plane bending vibrations are in the regions of 2975-2840/1470-1370 cm^{-1}, respectively [23].

M. Alam et al., [23] assigned the β_{CH}/τ_{C-H} modes in the ranges of 1549-1180cm^{-1}/906-773cm^{-1}, respectively for TDP molecule. In this study, based on the above conclusion the harmonic bands 1595, 1489, 1457, 1391, 1271, 1185 mode nos:17, 22, 24, 31, 37, 42) with considerable PED value(>20%) are assigned to β_{C-H} modes. The mode nos:22, 24, 37, 42 are in moderate agreement with literature value [23] in addition to experimental values: 1512, 1464, 1271 (FTIR), 1190cm^{-1} (FT-Raman). Similarly the calculated value of τ_{C-H} modes of perimidine ring are: 935, 840, 821, 794, 737, 725cm^{-1} (mode nos: 59, 63, 65, 67, 72, 73), in which mode nos:65, 67 are agreement with observed spectral values (822:FTIR, 797cm^{-1}:FT-Raman). These assignments also having considerable PED (>20%) value. Besides the νC_{21}-H_{22}, βC_{21}-H_{22} and τC_{21}-H_{22} deformation vibrations are attributed to mode nos: 16, and 38. On comparing ν_{C-H}, these assignments with literature value (νC-H: 2935cm^{-1}, βC-H: 1340) is negatively ~159cm^{-1} deviated. This is due to attachment of o-methoxy phenyl with C_{21} atom.

O–CH_3 group vibrations:

In methoxy group the C–H stretching bands were observed at 2977, 2828, 2838 cm^{-1}/2971, 2929, 2838 cm^{-1} in FT-IR/FT-Raman spectra are assigned to C–H asymmetric/ symmetric stretching modes,

respectively [36]. The stretching mode of O–CH_3 was assigned in the region of 1000–1100 cm^{-1} for anisole and its derivatives by some workers [37–40]. In this study, the O–CH_3 stretching mode observed at 1030/FT-IR cm^{-1} and its corresponding calculated value is 1017 cm^{-1} (mode no: 54). This assignment is further supported by PED value (72%).

Literature survey [37, 40] revealed that the C-O-CH_3 angle bending mode have been assigned in the region of 300-670cm^{-1} for anisole and its derivatives. [36] assigned this mode at 344cm^{-1} (FT-Raman) in the case of 4-methoxy-2-methyl benzoic acid. In accordance with above facts, the band observed at 494 cm^{-1} in FTIR and its corresponding harmonic value 487 cm^{-1} (mode no:85) is assigned to C-O-CH_3 angle bending mode. This mode lies in the region of ring planar C-C-C angle bending modes. In this study, a strong mixing of $\tau C_{25}C_{28}C_{26}C_{30}$ mode with the C-O-CH_3 angle bending mode. This trend is supported by literature [36].

Meganathan et al [36] assigned the torsional mode of the O–CH_3 group at 54 cm^{-1} in FT-Raman spectrum. In this study, the harmonic value 41 cm^{-1}/ mode no: 103 assigned to the O–CH_3 torsional mode. These assignments are having considerable PED values (27, 31%).

C-N Vibrations:

Generally the $\nu_{C=N}/\nu_{C-N}$ vibrations were observed in the regions of 1600–1670 cm^{-1} /1266-1382cm^{-1} [34,41]. According to the work by Z.Li and W. Deng [23] on 1′,3′-dihydrospiro [fluorine-9,2′-perimidine], the harmonic/observed wavenumber 1611/1623cm^{-1} : FTIR are assigned to ν_{C-N} mode. The C=N (aromatic) stretching mode appeared in the region 1490-1570 cm^{-1} khalaji et al., 2010 [42].

The C-N stretching vibrations are assigned to harmonic wavenumbers :1586, 1219, 956, 851cm^{-1} (mode nos:18, 41, 57, 62), in which mode nos:18, 41, 62 are in agreement with the observed FTIR bands:1589 (1591: FT-Raman), 1212, 863 cm^{-1}. These assignments are supported by their PED values. Besides, the observed FTIR bands: 1497, 1287cm^{-1} were assigned to ν_{C-N} mode for TDP [23]. The assigned ν_{C-N} modes are negatively/positively deviated from the literature values, which is due to the possibility of C-N bond polarization in the present molecule.

The in-plane bending vibrations: $\beta C_3C_2N_{17}$; $\beta N_{17}C_{21}N_{18}$ and $\beta C_8N_{18}C_{21}$ are attributed to mode nos:64, 79; 71, 89, and 81, 84 respectively. The out-of-plane bending mode of Γ_{C-N} contributes as mixed vibrations of $\Gamma C_1C_3N_{17}C_2$ (mode nos: 88, 91). While comparing, the recorded values for mode nos: 81/88 lie at 558/448cm^{-1} (FTIR bands) and 551/446cm^{-1} as harmonic frequencies which contribute about 45/52% of PED.

C–O vibrations:

In C-O group, the absorption is sensitive for both the carbon and oxygen atoms. Normally the C–O stretching vibration occurs in the region 1000–1260 cm^{-1} [36]. Meganathan et al., 2010 have assigned at 1251 cm^{-1} (FTIR) and 1248 cm^{-1} (FT-Raman) to aforementioned band. The intensity of the carbonyl group increases, due to the conjugation (or) formation of hydrogen bonds. The increase in conjugation, which increase the intensity of Raman lines as well as the IR band intensities [43]. According to the above facts, the harmonic frequencies 1228, 1017 (mode nos:40, 54) are designated as νC_{30}-O_{33}, νC_{34}-O_{33} modes, respectively with considerable PED values (59, 72%) as well as relative IR intensities (127.37, 30. 98). The mode no:54 is further supported by observed FTIR band: 1030cm^{-1} with medium intensity.

The in-plane bending vibrations of β_{C-O} are observed as mixed vibration of $\beta C_{28}C_{30}O_{33}$ at 797 cm^{-1} in FT-Raman spectrum, whereas the calculated frequencies are: 794, 737 (mode nos: 67, 72). Similarly, the C-O out-of-plane bending modes are also contribute as mixed vibration of $\Gamma O_{33}C_{26}C_{28}C_{30}$ at 494cm^{-1} in FT-IR and the harmonic frequencies are:511, 487 (mode nos: 83, 85). These assignments are having >26% of PED and also find support from literature [36].

C-C Vibrations:

The carbon–carbon (C-C) stretching vibrations were reported in the regions of 1625–1590, 1590–1575, 1540–1470, 1465–1430 and 1380–1280 cm^{-1} with variable intensity by Varsanyi [44]. In this study, the bands observed at 1544, 1365, 1271 cm^{-1} in FTIR and at 1280 in FT-Raman spectra are attributed to vC-C mode for phenyl ring in MPDP and their corresponding harmonic frequencies are: 1554, 1484, 1404, 1379, 1280, 1271 (mode nos :21, 23, 30, 32, 36, 37). The PED value corresponding to all v_{C-C} modes lie in between 20 and 68% and also mixed with β_{CH} mode. The ring breathing, in-plane and out-of-plane bending modes belong to phenyl ring were assigned at 726 (FT-Raman), 694 and 235cm^{-1} in FTIR spectrum, respectively [36]. The observed FTIR band at 756cm^{-1} (harmonic: 761cm^{-1}/mode no:70) is assigned to ring breathing mode and moderately in agreement with above literature value. Similarly, the theoretically calculated frequencies 624, 616 and 487, 247 (mode nos: 77, 78 and 85, 95) are belong to β_{CCC} and Γ_{CCC} modes, respectively. These assignments are further supported by PED value (>16%).

Alam and Lee [23] assigned the stretching vibrations of C-C in the wavenumber range 1180-1771cm^{-1} (FTIR) for TDP. The theoretically calculated v_{C-C} modes:1562-1065cm^{-1} (mode nos:20, 22, 27, 31-33, 39, 41, 42, 50, 52) have been obtained to be consistent with the recorded spectral values:1512, 1428, 1365, 1212 cm^{-1} (FTIR bands) and 1190, 1077cm^{-1} (FT-Raman). The β_{CCC} and τ_{CCC} modes were assigned at 796, 522 and 773, 471cm^{-1}, respectively for TDP [23]. Based on the above literature value, the harmonic frequencies in the ranges of 827-455cm^{-1} (64, 66, 69, 71, 79, 87) and 616-138cm^{-1} (78, 79, 82, 87, 100) are assigned to β_{CCC} and Γ_{CCC} modes of dyhydro perimidine ring, respectively. These assignments are in agreement with literature [23] and also having considerable PED values. (>33%: v_{CC}; >18%: β_{CCC}; >15%: Γ_{CCC}). The $vC_{21}C_{23}$, $\beta C_{21}C_{23}C_{25}$ and $\Gamma C_{21}C_{23}C_{25}C_{24}$ modes are assigned to mode nos: 43, 66 and 61, respectively. According to PED results the β_{CCC} and Γ_{CCC} vibrations are mixed with β_{CH} mode.

Nonlinear optical effects (NLO)

The NLO materials have recently attracted much interest because they involve new scientific phenomena and also they offer potential applications in emerging optoelectronic technologies, telecommunications, information storage, optical switching and signal processing [45]. The output from GAUSSIAN 03W provides 10 components of the 3x3x3 matrix as βxxx; βxxy; βxyy; βyyy; βxxz; βxyz; βyyz; βxzz; βyzz; βzzz; respectively. The total static dipole moment (μ), polarizability (α_0), and the first hyperpolarizability (β_0) can be calculated by using the following equations,

The dipole moment, polarizability and the first hyperpolarizability were calculated using B3LYP/6-311++G(d,p) basis set. As can be seen from Table 4, the calculated values of electronic dipole moment (μ), polarizability (α_0), and the first hyperpolarizability (β_0) are 1.3385 Debye, 0.6255x10^{-30} esu and 3.0847x10^{-30} esu, respectively. The first order hyper polarizability (β_0) value is 18 times greater than that of urea and hence the molecule has good NLO property.

NBO analysis:

The non-covalent bonding and anti-bonding interaction can be quantitatively described in terms of the NBO analysis, which is expressed by means of the second-order perturbation interaction energy ($E^{(2)}$) [46-49] 47–50]. This energy represents the estimation of the

$$\mu = (\mu_x^2 + \mu_y^2 + \mu_z^2)^{1/2} \qquad (2)$$

$$\alpha_0 = \frac{\alpha_{xx} + \alpha_{yy} + \alpha_{zz}}{3} \qquad (3)$$

$$\Delta\alpha = 2^{-1/2}\left[(\alpha_{xx} - \alpha_{yy})^2 + (\alpha_{yy} - \alpha_{zz})^2 + (\alpha_{zz} - \alpha_{xx})^2 + 6(\alpha_{xy}^2 + \alpha_{yz}^2 + \alpha_{xz}^2)\right]^{1/2} \qquad (4)$$

$$\beta_0 = (\beta_x^2 + \beta_y^2 + \beta_z^2)^{1/2} \qquad (5)$$

Table 4. The NLO measurements of MPDP

Parameters	B3LYP/6-311++G(d,p)
Dipole moment (μ)	**Debye**
μ_x	-1.3379
μ_y	0.00007
μ_z	-0.0385
μ	1.3385**Debye**
Polarizability (α$_0$)	***x10^{-30}esu***
α_{xx}	343.81
α_{xy}	0.00
α_{yy}	228.13
α_{xz}	-0.72
α_{yz}	-0.00
α_{zz}	160.95
α$_0$	0.62559**x10^{-30}esu**
Hyperpolarizability (β$_0$)	***x10^{-30}esu***
β_{xxx}	366.33
β_{xxy}	0.01
β_{xyy}	-44.56
β_{yyy}	0.02
β_{xxz}	100.48
β_{xyz}	0.00
β_{yyz}	-14.30
β_{xzz}	1.72
β_{yzz}	-0.01
β_{zzz}	64.94
β$_0$	3.08470**x10^{-30}esu**

Standard value for urea (**μ**=1.3732 Debye, **β$_0$**=0.3728x10^{-30}esu): **esu**-electrostatic unit

off-diagonal NBO Fock matrix elements. It can be deduced from the second-order perturbation approach [50]:

where qi is the donor orbital occupancy, Σi and Σj are diagonal elements (orbital energies) and F(i, j) is off diagonal NBO Fock matrix elements.

NBO analysis was performed by the B3LYP/6-311++G(d,p) basis set for the molecule MPDP and are listed in Table 5. The intramolecular hyperconjugative interactions energes are formed by the orbital overlap between π(C–C) and π*(C–C) bond orbitals, which results intra molecular charge transfer (ICT) causing stabilization of the system.

In perimidine moiety, the orbitals interaction between π(C_1-C_2)→π* (C_5-C_6), π(C_5-C_6)→ π*(C_3-C_4), π (C_8-C_{13})→π*(C_9-C_{12}), π(C_9-C_{12})→π*(C_3-C_4), which

$$E^{(2)} = \Delta E_{ij} = q_i \frac{F(i,j)^2}{\varepsilon_j - \varepsilon_i} \qquad (6)$$

transfer higher energy: 88.99, 80.63, 88.95, 80.54 KJ/ mol, respectively and hence stabilization increases. It is noted from the Table--- that there occur a strong intra-molecular hyperconjugative interactions of C_1-C_2 and C_{13} -C_{18} from π(C_3-C_4) → π*(C_1-C_2) / (C_8-C_{13}), which increase electron density (ED) 0.3377 and 0.3379 e) that weakens the respective bands C_1-C_2 and C_8-C_{13} leading to the stabilization of 95.1 and 95.23KJ/mol, respective-ly. The anti-bonding orbitals (C_1-C_2) and (C_{13}-C_8) are attached with N_{17} and N_{18} atoms, respectively, which also enhances the EDs due to resonance structure of the compound.

Similarly in benzene ring, the strong intra-molecular hyperconjugative interactions: π(C_{23}-C_{24})→π* (C_{25}-C_{28}), π(C_{25}-C_{28})→π*(C_{26}-C_{30}), π(C_{26}-C_{30})→π*(C_{23}-C_{24}), which increase the electron densities (EDs): (0.3395, 0.3822, 0.3528e), that weaken the respective bonds and hence the stabilization increases 86.73, 88. 99, 84.22 KJ/mol, respectively.

The lone pair of oxygen and nitrogen atoms play great role in the MPDP molecule. During n→π* transitions:LpN_{17}→π* (C_1-C_2) and LpN_{18}→π* (C_8-C_{13}) more energy delocalization take place and their corresponding excitation energy values are: 70.21 and 70.17KJ/mol, respectively. Besides the Lp O_{33} atom transfer energy: 77.86KJ/mol to anti-bonding orbital π* (C_{26}-C_{30}) on comparing with π* (C_{28}-C_{30}) transition: 5.36KJ/mol. This is due to the lone pair electrons of oxygen in methoxy group may be involved in energy state. So that abnormal energy is appeared. The maximum hyperconjugative $E^{(2)}$ energy of heteroatoms during the intra-molecular interaction leads the molecule

Table 5. The second order perturbation theory analysis of Fock Matrix in NBO basis for MPDP

Type	Donor NBO (i)	ED/e	Acceptor NBO (j)	ED/e	$E^{(2)}$ KJ/mol	E(j)-E(i) a.u.	F(i,j) a.u.
σ -σ*	BD (1) C 1 - C 2	1.97745	BD*(1) C 1 - C 6	0.01374	10.5	1.27	0.05
			BD*(1) C 1 - H 7	0.01199	5.61	1.19	0.036
			BD*(1) C 2 - C 3	0.02874	17.66	1.28	0.066
			BD*(1) C 3 - C 8	0.02874	12.84	1.28	0.056
			BD*(1) C 6 - H 11	0.01105	8.45	1.2	0.044
			BD*(1) N 17 - C 21	0.02799	5.73	1.03	0.034
π -π*	BD (2) C 1 - C 2	1.70554	BD*(2) C 3 - C 4	0.5074	63.18	0.3	0.063
			BD*(2) C 5 - C 6	0.29421	88.99	0.29	0.07
σ -σ*	BD (1) C 1 - C 6	1.97803	BD*(1) C 1 - C 2	0.01907	12.22	1.26	0.054
			BD*(1) C 1 - H 7	0.01199	5.86	1.18	0.036
			BD*(1) C 2 - N 17	0.02361	17.74	1.04	0.059
			BD*(1) C 5 - C 6	0.01359	9.83	1.26	0.049
			BD*(1) C 5 - H 10	0.01155	9.41	1.19	0.046
			BD*(1) C 6 - H 11	0.01105	4.77	1.19	0.033
σ -σ*	BD (1) C 1 - H 7	1.98106	BD*(1) C 1 - C 2	0.01907	4.35	1.1	0.03
			BD*(1) C 2 - C 3	0.02874	17.82	1.11	0.062
			BD*(1) C 5 - C 6	0.01359	13.85	1.1	0.054
σ -σ*	BD (1) C 2 - C 3	1.96808	BD*(1) C 1 - C 2	0.01907	14.94	1.27	0.06
			BD*(1) C 1 - H 7	0.01199	8.24	1.19	0.043
			BD*(1) C 3 - C 4	0.03301	19.04	1.29	0.068
			BD*(1) C 3 - C 8	0.02874	17.49	1.28	0.065
			BD*(1) C 4 - C 9	0.0215	10.46	1.28	0.051
			BD*(1) C 8 - C 13	0.01908	10.71	1.27	0.051
			BD*(1) N 17 - H 19	0.01237	4.39	1.18	0.032
σ -σ*	BD (1) C 2 - N 17	1.98308	BD*(1) C 1 - C 6	0.01374	6.74	1.29	0.041
			BD*(1) C 2 - C 3	0.02874	4.23	1.3	0.032
			BD*(1) C 3 - C 4	0.03301	9.79	1.31	0.05
			BD*(1) C 21 - C 23	0.03162	8.16	1.11	0.042
σ -σ*	BD (1) C 3 - C 4	1.95847	BD*(1) C 2 - C 3	0.02874	19.54	1.26	0.069
			BD*(1) C 2 - N 17	0.02361	15.23	1.04	0.055
			BD*(1) C 3 - C 8	0.02874	19.54	1.26	0.069
			BD*(1) C 4 - C 5	0.0215	14.56	1.26	0.06
			BD*(1) C 4 - C 9	0.0215	14.56	1.26	0.06
			BD*(1) C 5 - H 10	0.01155	7.87	1.19	0.043
			BD*(1) C 8 - N 18	0.02365	15.23	1.04	0.055
			BD*(1) C 9 - H 14	0.01154	7.87	1.19	0.043
π -π*	BD (2) C 3 - C 4	1.5483	BD*(2) C 1 - C 2	0.3377	95.1	0.27	0.072
			BD*(2) C 5 - C 6	0.29421	63.55	0.28	0.06
			BD*(2) C 8 - C 13	0.33793	95.23	0.27	0.072
			BD*(2) C 9 - C 12	0.29421	63.64	0.28	0.06
σ -σ*	BD (1) C 3 - C 8	1.96807	BD*(1) C 1 - C 2	0.01907	10.71	1.27	0.051
			BD*(1) C 2 - C 3	0.02874	17.45	1.28	0.065
			BD*(1) C 3 - C 4	0.03301	19.04	1.29	0.068
			BD*(1) C 4 - C 5	0.0215	10.46	1.28	0.051
			BD*(1) C 8 - C 13	0.01908	14.94	1.27	0.06
			BD*(1) C 13 - H 16	0.01201	8.24	1.19	0.043
			BD*(1) N 18 - H 20	0.0124	4.39	1.18	0.032

Table 5 continued from page 22

Type	Donor NBO (i)	ED/e	Acceptor NBO (j)	ED/e	$E^{(2)}$ KJ/mol	E(j)-E(i) a.u.	F(i,j) a.u.
σ -σ*	BD (1) C 4 - C 5	1.97357	BD*(1) C 3 - C 4	0.03301	17.2	1.27	0.065
			BD*(1) C 3 - C 8	0.02874	13.14	1.26	0.056
			BD*(1) C 4 - C 9	0.0215	14.81	1.26	0.06
			BD*(1) C 5 - C 6	0.01359	9.75	1.26	0.048
			BD*(1) C 5 - H 10	0.01155	4.9	1.18	0.033
			BD*(1) C 6 - H 11	0.01105	9	1.19	0.045
			BD*(1) C 9 - C 12	0.01359	8.2	1.26	0.044
σ -σ*	BD (1) C 4 - C 9	1.97358	BD*(1) C 2 - C 3	0.02874	13.14	1.26	0.056
			BD*(1) C 3 - C 4	0.03301	17.15	1.27	0.065
			BD*(1) C 4 - C 5	0.0215	14.81	1.26	0.06
			BD*(1) C 5 - C 6	0.01359	8.2	1.26	0.044
			BD*(1) C 9 - C 12	0.01359	9.75	1.26	0.048
			BD*(1) C 9 - H 14	0.01154	4.9	1.18	0.033
			BD*(1) C 12 - H 15	0.01106	9.04	1.19	0.045
σ -σ*	BD (1) C 5 - C 6	1.98099	BD*(1) C 1 - C 6	0.01374	9.87	1.25	0.049
			BD*(1) C 1 - H 7	0.01199	9.96	1.17	0.047
			BD*(1) C 4 - C 5	0.0215	11	1.26	0.051
			BD*(1) C 4 - C 9	0.0215	13.43	1.26	0.057
			BD*(1) C 5 - H 10	0.01155	5.56	1.18	0.035
			BD*(1) C 6 - H 11	0.01105	5.19	1.18	0.034
π -π*	BD (2) C 5 - C 6	1.73017	BD*(2) C 1 - C 2	0.3377	70.46	0.28	0.062
			BD*(2) C 3 - C 4	0.5074	80.63	0.29	0.071
σ -σ*	BD (1) C 5 - H 10	1.98208	BD*(1) C 1 - C 6	0.01374	14.1	1.09	0.054
			BD*(1) C 3 - C 4	0.03301	18.95	1.11	0.064
			BD*(1) C 4 - C 5	0.0215	4.77	1.1	0.032
σ -σ*	BD (1) C 6 - H 11	1.98314	BD*(1) C 1 - C 2	0.01907	15.36	1.1	0.057
			BD*(1) C 4 - C 5	0.0215	14.48	1.11	0.055
σ -σ*	BD (1) C 8 - C 13	1.97744	BD*(1) C 2 - C 3	0.02874	12.84	1.28	0.056
			BD*(1) C 3 - C 8	0.02874	17.66	1.28	0.066
			BD*(1) C 12 - C 13	0.01375	10.5	1.27	0.05
			BD*(1) C 12 - H 15	0.01106	8.45	1.2	0.044
			BD*(1) C 13 - H 16	0.01201	5.65	1.19	0.036
			BD*(1) N 18 - C 21	0.02797	5.73	1.03	0.034
π -π*	BD (2) C 8 - C 13	1.70593	BD*(2) C 3 - C 4	0.5074	63.09	0.3	0.063
			BD*(2) C 9 - C 12	0.29421	88.95	0.29	0.07
σ -σ*	BD (1) C 8 - N 18	1.98309	BD*(1) C 3 - C 4	0.03301	9.79	1.31	0.05
			BD*(1) C 3 - C 8	0.02874	4.23	1.3	0.032
			BD*(1) C 12 - C 13	0.01375	6.74	1.29	0.041
			BD*(1) C 21 - C 23	0.03162	8.12	1.11	0.042
σ -σ*	BD (1) C 9 - C 12	1.98098	BD*(1) C 4 - C 5	0.0215	13.39	1.26	0.057
			BD*(1) C 4 - C 9	0.0215	11	1.26	0.051
			BD*(1) C 9 - H 14	0.01154	5.56	1.18	0.035
			BD*(1) C 12 - C 13	0.01375	9.92	1.25	0.049
			BD*(1) C 12 - H 15	0.01106	5.19	1.18	0.034
			BD*(1) C 13 - H 16	0.01201	9.96	1.17	0.047
π -π*	BD (2) C 9 - C 12	1.73041	BD*(2) C 3 - C 4	0.5074	80.54	0.29	0.071
			BD*(2) C 8 - C 13	0.33793	70.46	0.28	0.062
σ -σ*	BD (1) C 9 - H 14	1.98207	BD*(1) C 3 - C 4	0.03301	18.95	1.11	0.064
			BD*(1) C 4 - C 9	0.0215	4.77	1.1	0.032
			BD*(1) C 12 - C 13	0.01375	14.1	1.09	0.054

Table 5 continued from page 23

Type	Donor NBO (i)	ED/e	Acceptor NBO (j)	ED/e	$E^{(2)}$ KJ/mol	E(j)-E(i) a.u.	F(i,j) a.u.
σ -σ*	BD (1) C 12 - C 13	1.97803	BD*(1) C 8 - C 13	0.01908	12.22	1.26	0.054
			BD*(1) C 8 - N 18	0.02365	17.74	1.04	0.059
			BD*(1) C 9 - C 12	0.01359	9.83	1.26	0.049
			BD*(1) C 9 - H 14	0.01154	9.41	1.19	0.046
			BD*(1) C 12 - H 15	0.01106	4.77	1.19	0.033
			BD*(1) C 13 - H 16	0.01201	5.86	1.18	0.036
σ -σ*	BD (1) C 12 - H 15	1.98314	BD*(1) C 4 - C 9	0.0215	14.48	1.11	0.055
			BD*(1) C 8 - C 13	0.01908	15.36	1.1	0.057
σ -σ*	BD (1) C 13 - H 16	1.98107	BD*(1) C 3 - C 8	0.02874	17.82	1.11	0.062
			BD*(1) C 8 - C 13	0.01908	4.35	1.1	0.03
			BD*(1) C 9 - C 12	0.01359	13.81	1.1	0.054
σ -σ*	BD (1) N 17 - H 19	1.97746	BD*(1) C 2 - C 3	0.02874	13.47	1.22	0.056
			BD*(1) N 18 - C 21	0.02797	14.23	0.97	0.051
σ -σ*	BD (1) N 17 - C 21	1.98137	BD*(1) C 1 - C 2	0.01907	10.59	1.28	0.051
			BD*(1) N 18 - H 20	0.0124	6.15	1.19	0.037
			BD*(1) C 23 - C 24	0.02096	7.53	1.28	0.043
σ -σ*	BD (1) N 18 - H 20	1.97748	BD*(1) C 3 - C 8	0.02874	13.43	1.22	0.056
			BD*(1) N 17 - C 21	0.02799	14.18	0.97	0.051
σ -σ*	BD (1) N 18 - C 21	1.98135	BD*(1) C 8 - C 13	0.01908	10.59	1.28	0.051
			BD*(1) N 17 - H 19	0.01237	6.15	1.19	0.037
			BD*(1) C 23 - C 25	0.02102	7.53	1.28	0.043
σ -π*	BD (1) C 21 - H 22	1.98147	BD*(2) C 23 - C 24	0.3528	12.09	0.56	0.039
σ -σ*	BD (1) C 21 - C 23	1.97233	BD*(1) C 2 - N 17	0.02361	8.87	0.98	0.041
			BD*(1) C 8 - N 18	0.02365	8.87	0.98	0.041
			BD*(1) C 23 - C 24	0.02096	7.07	1.18	0.04
			BD*(1) C 23 - C 25	0.02102	7.11	1.18	0.04
			BD*(1) C 24 - C 26	0.01485	9.25	1.19	0.046
			BD*(1) C 25 - C 28	0.0129	9.08	1.18	0.045
σ -σ*	BD (1) C 23 - C 24	1.97551	BD*(1) C 21 - C 23	0.03162	6.9	1.09	0.038
			BD*(1) C 23 - C 25	0.02102	15.73	1.27	0.062
			BD*(1) C 24 - C 26	0.01485	11.59	1.27	0.053
			BD*(1) C 24 - H 27	0.01386	5.73	1.19	0.036
			BD*(1) C 25 - H 29	0.01346	8.87	1.19	0.045
			BD*(1) C 26 - H 31	0.01551	9.12	1.19	0.046
π -σ*	BD (2) C 23 - C 24	1.6656	BD*(1) N 17 - C 21	0.02799	6.19	0.58	0.029
			BD*(1) C 21 - H 22	0.04118	9.41	0.74	0.04
			BD*(2) C 25 - C 28	0.33945	86.73	0.28	0.068
			BD*(2) C 26 - C 30	0.38222	80.63	0.27	0.065
σ -σ*	BD (1) C 23 - C 25	1.97568	BD*(1) C 21 - C 23	0.03162	6.9	1.09	0.038
			BD*(1) C 23 - C 24	0.02096	15.77	1.27	0.062
			BD*(1) C 24 - H 27	0.01386	8.95	1.19	0.045
			BD*(1) C 25 - C 28	0.0129	11.05	1.26	0.052
			BD*(1) C 25 - H 29	0.01346	5.77	1.19	0.036
			BD*(1) C 28 - H 32	0.01141	8.49	1.19	0.044

Table 5 continued from page 24

Type	Donor NBO (i)	ED/e	Acceptor NBO (j)	ED/e	$E^{(2)}$ KJ/mol	E(j)-E(i) a.u.	F(i,j) a.u.
σ -σ*	BD (1) C 24 - C 26	1.97407	BD*(1) C 21 - C 23	0.03162	14.77	1.09	0.055
			BD*(1) C 23 - C 24	0.02096	13.47	1.26	0.057
			BD*(1) C 24 - H 27	0.01386	5.86	1.18	0.036
			BD*(1) C 26 - C 30	0.0264	12.09	1.25	0.054
			BD*(1) C 26 - H 31	0.01551	6.61	1.19	0.039
			BD*(1) C 30 - O 33	0.03116	16.61	0.99	0.056
σ -σ*	BD (1) C 24 - H 27	1.97987	BD*(1) N 18 - H 20	0.0124	4.48	1.02	0.03
			BD*(1) C 23 - C 24	0.02096	5.27	1.11	0.033
			BD*(1) C 23 - C 25	0.02102	16.95	1.11	0.06
			BD*(1) C 26 - C 30	0.0264	14.27	1.09	0.055
σ -σ*	BD (1) C 25 - C 28	1.97445	BD*(1) C 21 - C 23	0.03162	14.94	1.09	0.056
			BD*(1) C 23 - C 25	0.02102	13.22	1.26	0.056
			BD*(1) C 25 - H 29	0.01346	5.69	1.18	0.036
			BD*(1) C 28 - C 30	0.02221	10.42	1.25	0.05
			BD*(1) C 28 - H 32	0.01141	5.56	1.19	0.036
			BD*(1) C 30 - O 33	0.03116	18.45	0.98	0.059
π -π*	BD (2) C 25 - C 28	1.68745	BD*(2) C 23 - C 24	0.3528	83.05	0.28	0.068
			BD*(2) C 26 - C 30	0.38222	88.99	0.27	0.069
σ -σ*	BD (1) C 25 - H 29	1.97956	BD*(1) N 17 - H 19	0.01237	4.48	1.02	0.03
			BD*(1) C 23 - C 24	0.02096	17.07	1.11	0.06
			BD*(1) C 23 - C 25	0.02102	5.27	1.11	0.033
			BD*(1) C 28 - C 30	0.02221	14.1	1.1	0.054
σ -σ*	BD (1) C 26 - C 30	1.98073	BD*(1) C 24 - C 26	0.01485	11.51	1.28	0.053
			BD*(1) C 24 - H 27	0.01386	9.12	1.2	0.046
			BD*(1) C 26 - H 31	0.01551	6.23	1.2	0.038
			BD*(1) C 28 - C 30	0.02221	14.23	1.27	0.059
			BD*(1) C 28 - H 32	0.01141	8.54	1.21	0.044
π -π*	BD (2) C 26 - C 30	1.6575	BD*(2) C 23 - C 24	0.3528	84.22	0.29	0.069
			BD*(2) C 25 - C 28	0.33945	78.91	0.29	0.066
σ -σ*	BD (1) C 26 - H 31	1.97659	BD*(1) C 23 - C 24	0.02096	14.43	1.11	0.055
			BD*(1) C 24 - C 26	0.01485	4.23	1.11	0.03
			BD*(1) C 26 - C 30	0.0264	4.48	1.09	0.031
			BD*(1) C 28 - C 30	0.02221	15.86	1.1	0.058
			BD*(1) C 34 - H 35	0.01969	4.52	1.01	0.03
σ -σ*	BD (1) C 28 - C 30	1.97936	BD*(1) C 25 - C 28	0.0129	9.75	1.28	0.049
			BD*(1) C 25 - H 29	0.01346	9.12	1.2	0.046
			BD*(1) C 26 - C 30	0.0264	13.97	1.26	0.058
			BD*(1) C 26 - H 31	0.01551	8.87	1.2	0.045
			BD*(1) C 28 - H 32	0.01141	5.86	1.21	0.037
			BD*(1) O 33 - C 34	0.00541	6.11	0.99	0.034
σ -σ*	BD (1) C 28 - H 32	1.97995	BD*(1) C 23 - C 25	0.02102	15.27	1.1	0.057
			BD*(1) C 26 - C 30	0.0264	16.9	1.08	0.059
σ -σ*	BD (1) C 30 - O 33	1.98907	BD*(1) C 24 - C 26	0.01485	5.94	1.39	0.04
			BD*(1) C 25 - C 28	0.0129	5.86	1.38	0.039
			BD*(1) C 34 - H 36	0.00893	5.94	1.3	0.038
σ -σ*	BD (1) O 33 - C 34	1.99038	BD*(1) C 28 - C 30	0.02221	11.63	1.35	0.055
σ -σ*	BD (1) C 34 - H 35	1.99375	BD*(1) C 26 - H 31	0.01551	6.02	1.04	0.035
σ -σ*	BD (1) C 34 - H 36	1.99106	BD*(1) C 30 - O 33	0.03116	11.55	0.83	0.043
n -π*	LP (1) N 17	1.86213	BD*(2) C 1 - C 2	0.3377	70.21	0.35	0.072
			BD*(1) N 18 - C 21	0.02797	7.24	0.65	0.031
			BD*(1) C 21 - H 22	0.04118	24.81	0.81	0.063
n -π*	LP (1) N 18	1.86229	BD*(2) C 8 - C 13	0.33793	70.17	0.35	0.072
			BD*(1) N 17 - C 21	0.02799	7.24	0.65	0.031
			BD*(1) C 21 - H 22	0.04118	24.81	0.81	0.063
n -σ*	LP (1) O 33	1.96907	BD*(1) C 26 - C 30	0.0264	21.13	1.13	0.068
			BD*(1) C 34 - H 35	0.01969	7.2	1.05	0.038
			BD*(1) C 34 - H 36	0.00893	4.98	1.07	0.032
n -π*	LP (2) O 33	1.87925	BD*(2) C 26 - C 30	0.38222	77.86	0.33	0.075
			BD*(1) C 28 - C 30	0.02221	5.36	0.87	0.031
			BD*(1) C 34 - H 35	0.01969	16.36	0.78	0.051
			BD*(1) C 34 - H 37	0.01677	23.97	0.79	0.062
π*-π*	BD*(2) C 1 - C 2	0.3377	BD*(2) C 3 - C 4	0.5074	1094.2	0.01	0.083
π*-π*	BD*(2) C 8 - C 13	0.33793	BD*(2) C 3 - C 4	0.5074	1081	0.01	0.083
π*-σ*	BD*(2) C 23 - C 24	0.3528	BD*(1) C 21 - H 22	0.04118	4.9	0.46	0.047
π*-π*	BD*(2) C 26 - C 30	0.38222	BD*(2) C 23 - C 24	0.3528	1114.1	0.01	0.079

towards medicinal and biological applications.

Homo-Lumo analysis

The frontier molecular orbitals play an important role in the optical and electric properties, as well as in quantum chemistry. The frontier molecular orbital gap also helps to characterize the chemical reactivity and the kinetic stability of the molecule. A molecule with a small frontier orbital gap is generally associated with high chemical reactivity and low kinetic stability and is also termed as soft molecule [51]. The calculated energy values of HOMO and LUMO in gas phase are -5.0725 and -1.0149eV, respectively, and the frontier orbital energy gap value is 3.0437eV. The frontier molecular orbitals (HOMO and LUMO) and their corresponding energies are shown in Fig. 5. physico chemical parameters are shown in Table 6. The density of state (DOS) of the present molecule has been plotted and shown in Fig.6. DOS denoted the number of available molecular orbitals at different energy.

UV–Vis analysis

The absorption wavelengths (λ), oscillator strengths (f), and excitation energies were calculated at TD-DFT/B3LYP/6-311++G(d,p) level. The UV–Vis spectrum of the MPDP was recorded in the wavelength range 200–800nm as shown in Fig. 7. The electronic spectrum of title molecule shows the transitions at 276nm and 327nm. In MPDP, the calculated UV absorption result has three excited states (ESs). The ES_1, ES_2, and ES_3 appeared at 342.36, 313.62 and 309.46 nm and their corresponding excitation energies are 3.6214, 3.9533 and 4.006eV, respectively. These bonds are due to transition HOMO→LUMO (88%), HOMO→LUMO-3(80%) and HOMO→LUMO-2(92%) in gaseous phase. The calculated band gap 309.46 nm of ES3 coincide with the recorded value of 276 nm. The excitation energies of MPDP are listed in Table.7.

Mulliken charges

The calculation of atomic charges plays an important role in the application of quantum mechanical

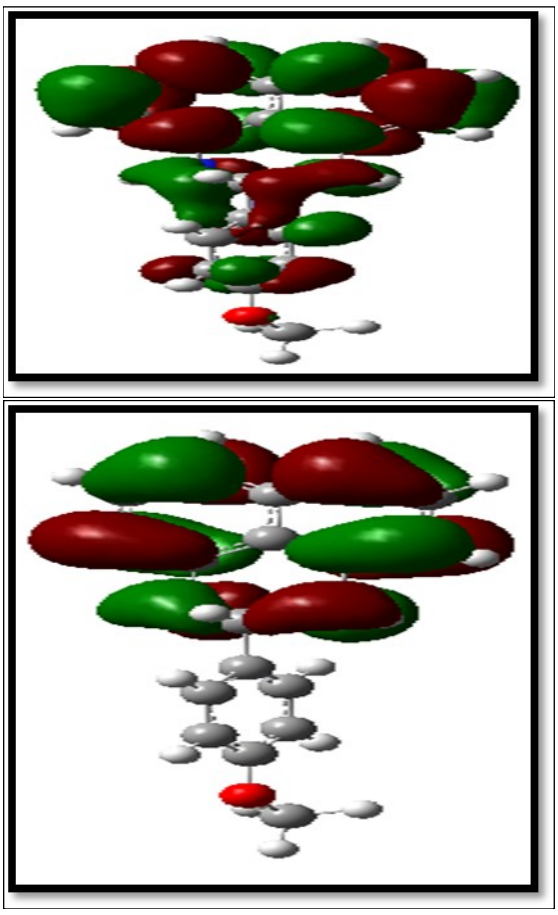

Fig. 5. The frontier molecular orbital diagram of MPDP

Table 6. The Physico-chemical properties of MPDP

Parameters	Values
HOMO	-5.072 eV
LUMO	-1.014 eV
Energy gap	3.043 eV
Ionization potential (IP)	-5.072 eV
Electron affinity (EA)	-1.014 eV
Electrophilicity Index (ω)	1.141
Chemical Potential (μ)	3.043
Electronegativity (χ)	-3.043eV
Hardness (η)	-3.043

calculations to molecular systems [52]. The charge distributions are calculated by Mulliken method using B3LYP/6-311++G(d,p) level of basis set for the equilibrium geometry of DPMP are given in Table. 8. The charge distribution on the molecule has an important influence on the vibrational spectra. The corresponding Mulliken's plot is shown in Fig. 8. The C_4 atom possess most positive charge, which is due to the formation of conjugation in perimidine ring. The C_{21} atom attached with two nitrogen atom in adjacent position. Due to the presence of lone pair of electrons on nitrogen atoms, the C_{21} atom has more negative charge among the other carbon atoms. All the hydrogen atoms have net positive charges.

MEP analysis

In the present study, 3D plots of molecular electrostatic potential (MEP) has been drawn in Fig. 9. The MEP is a plot of electrostatic potential mapped onto the constant ED surface. The different values of the electrostatic potential at the surface are represented by different colors. Potential increases in the order red < orange < yellow < green < blue. The color code of the MEP map is in the range between -9.517e-2 (deepest red) and 9.517e-2 (deepest blue) and the, blue colour represents the strongest attraction and red represents the strongest repulsion. The MEP map shows, the

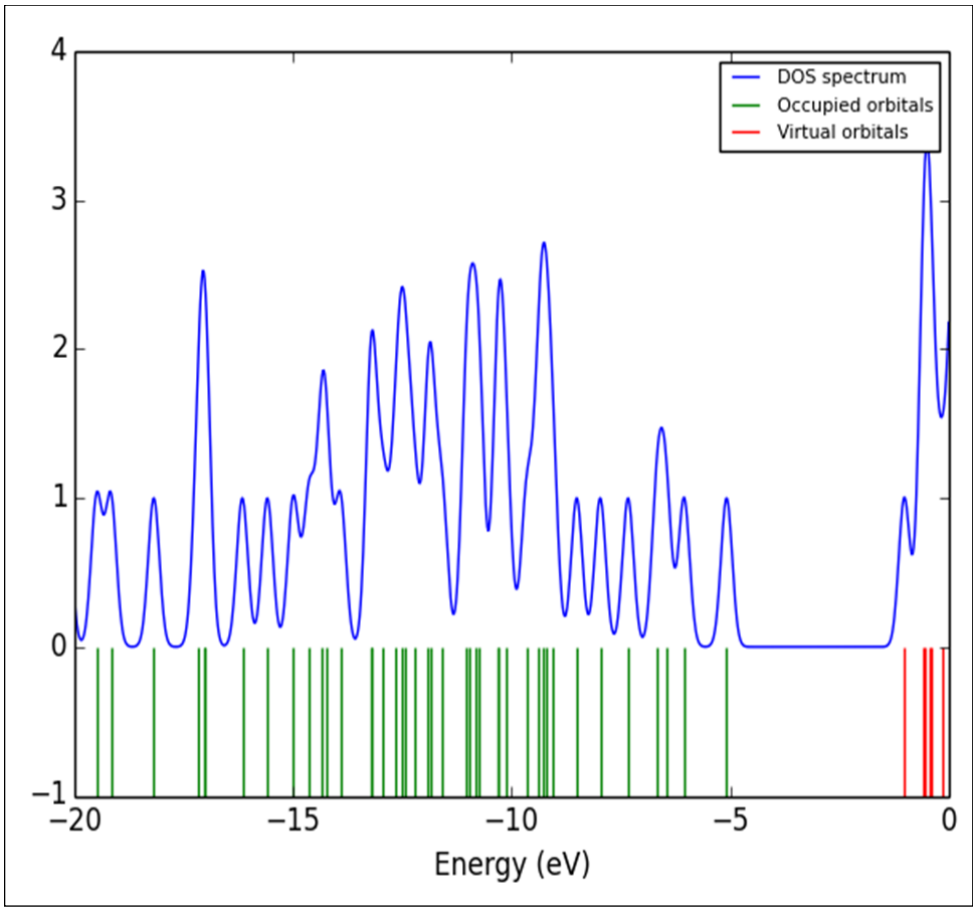

Fig.6. The Dos spectrum

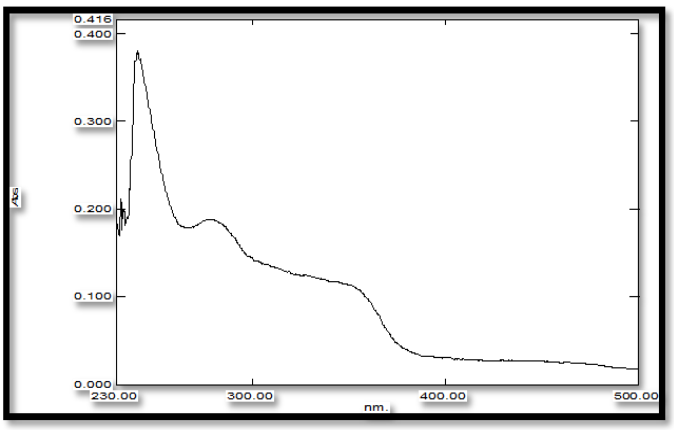

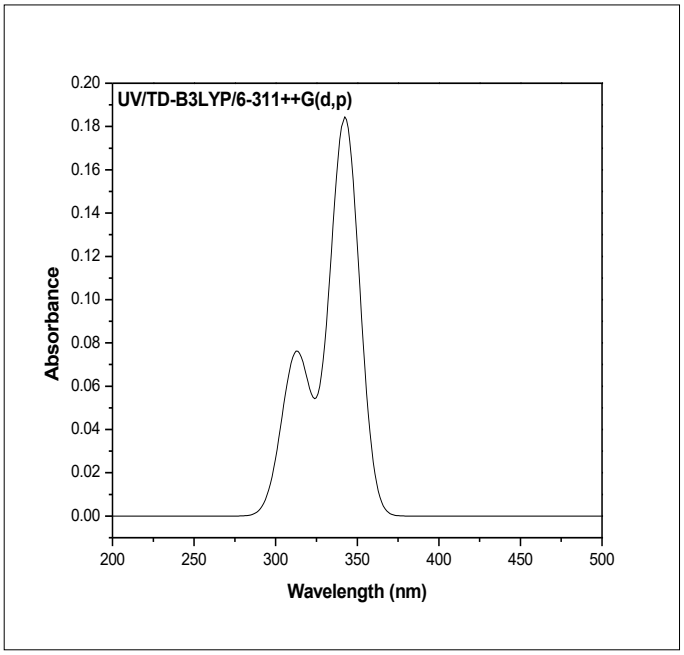

Fig. 7. Combined experimental and theoretical UV-Visible spectra of MPDP

Table 7. The electronic transitions of MPDP

Calculated at B3LYP/6-311++G (d,p)	Oscillator strength	Calculated Band gap(eV/nm)	Experimental Band gap (eV/nm)
Excited State 1 73 -> 74	Singlet-A(f=0.1842) 0.66291	3.6214 eV/342.36 nm 4.057476	327
Excited State 2 70 -> 74 70 -> 75 73 -> 76	Singlet-A(f=0.0611) -0.24099 0.12032 0.63209	3.9533 eV/313.62 nm -5.644712 6.062133 4.611499	
Excited State 3 3 -> 75 73 -> 77	Singlet-A(f=0.0160) 0.67644 -0.10991	4.0065 eV/309.46 nm 4.474898 -4.661295	276

Table 8. The Mulliken atomic charges of MPDP

Atoms	Charges
1C	-0.1527
2C	-0.2458
3C	0.3349
4C	0.4394
5C	-0.3593
6C	-0.1967
7H	0.1148
8C	-0.2458
9C	-0.3593
10H	0.1225
11H	0.1660
12C	-0.1968
13C	-0.1529
14H	0.1225
15H	0.1660
16H	0.1148
17N	0.2352
18N	0.2352
19H	0.2302
20H	0.2301
21C	-0.8104
22H	0.1968
23C	0.0076
24C	0.3594
25C	-0.1828
26C	0.1642
27H	0.1921
28C	-0.3033
29H	0.1628
30C	-0.7835
31H	0.2038
32H	0.2025
33O	-0.1541
34C	-0.3411
35H	0.1531
36H	0.1775
37H	0.1531

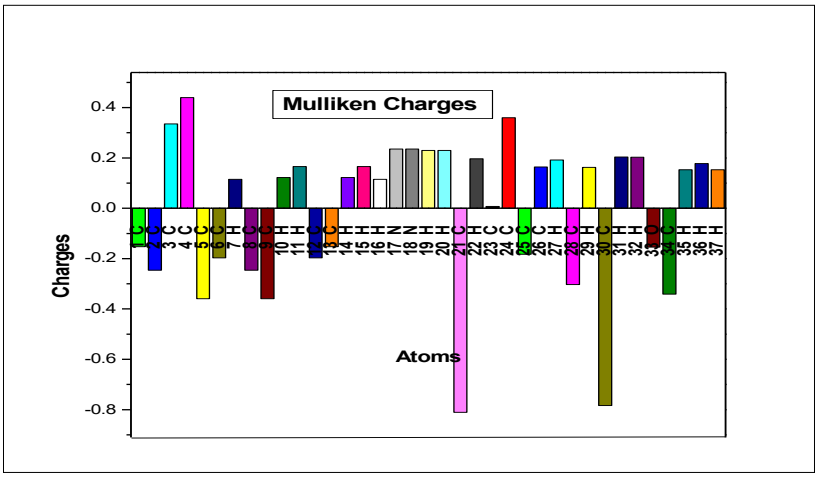

Fig 8. Mulliken atomic charges plot of MPDP

negative region is located on nitrogen atom in perimidine ring (red region) and the positive region (blue region) is located on the methoxy group is phenyl ring.

The red and blue areas in the MEP map refer to the regions of negative and positive potentials and correspond to the electron rich and electron-poor regions, respectively, whereas the green color denotes the neutral electrostatic potential. The MEP surface provides necessary information about the reactive sites.

Molecular docking:

Molecular docking study was carried out to study the precise binding site of ligand on protein. A molecular docking study is a key tool in structural molecular biology and computer assisted drug design. The synthesized analogue docking with crystal structure of human lanosterol 14-alpha dimethylase in complex with ketaconazole (3LD6). Analogue showed best ligand pose energy -13.23kcal/mol in 3LD6 protein. The protein ligand interactions are shown in Figure. 10. In compound MPDP surrounded by wander walls interaction of amino acids residues PHEB543, METB545, ALAB682, HISB681 and METB932. There are two alkyl interaction TRPB684 and LEUB685 inside the benzene ring. The pi-alkyl interaction in PHEB550, METB826, PHEB552, CYSB847, TYRB552 and ILEB824 perimidine inside the ring. From this interaction it can be predicted as the activity may be due to inhibition of human lanosterol 14-alpha dimethylase in complex with ketaconazole.

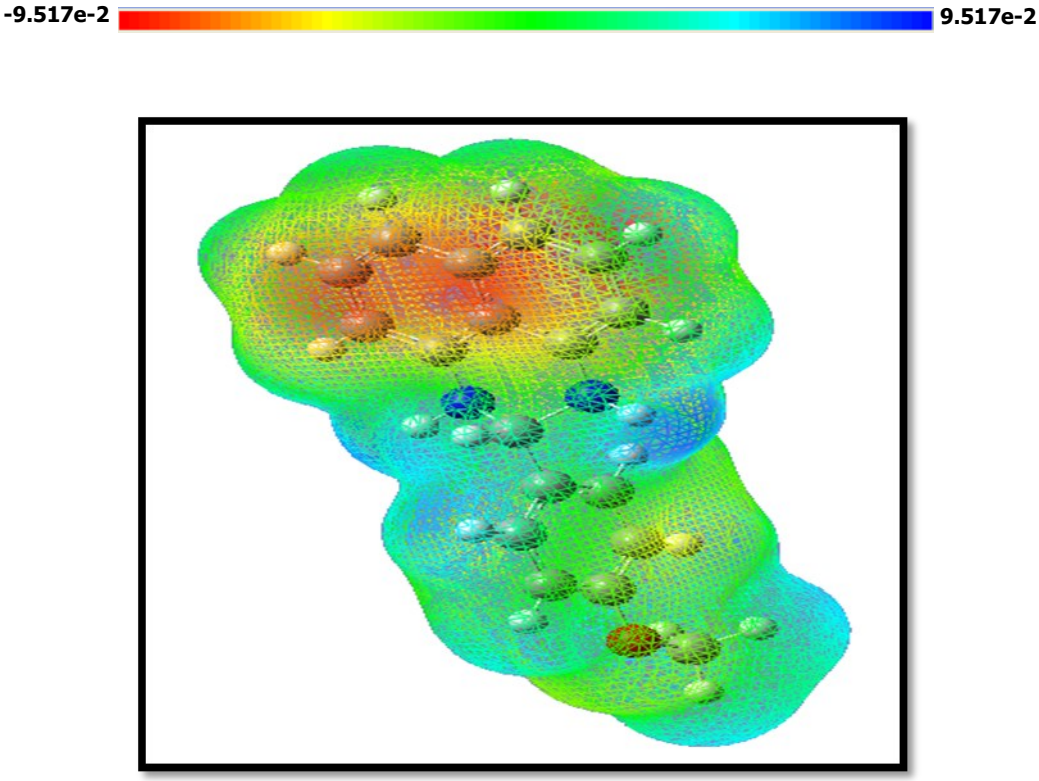

Fig. 9. MEP surfaces map of MPDP

Thermodynamic properties

The thermodynamic functions such as entropy (S), heat capacity at constant pressure (Cp) total and enthalpy (E) for different range (100–1000 K) of temperatures are determined and these results are presented in the Table. 9. The thermodynamic functions are increasing with temperature ranging from 100 to 1000 K due to the fact that the molecular vibrational intensities increase with temperature [53]. The correlation graph between thermodynamic functions and its different temperatures are graphically represented in Fig. 11. All the thermodynamic data supply helpful information for the further study on the molecule MPDP. They can be used to compute the other thermodynamic energies according to relationships of thermodynamic functions and estimate directions of chemical reactions according to the second law of thermodynamics in thermochemical field.

The corresponding fitting equations are as follows:

$C^0_{p,m} = 7.1574 + 0.0302T + 2.6697x10^{-5}\ T^2$ (R^2 = 0.9992)

$S^0_m = 3.3949 + 0.0143T + 1.2663x10^{-5}\ T^2$ (R^2 = 0.9999)

$\Delta H^0_m = 4.8494 + 0.0204T + 1.8089x10^{-5}\ T^2$ (R^2 = 0.9993)

All the given thermodynamic data are the helpful information for further study on MPDP. It can be used to compute the other thermodynamic energies according to relationships of thermodynamic functions and estimate directions of chemical reactions according to the second law of thermodynamics in thermochemical field [53]. All the thermodynamic calculations were done in gas phase and they could not be used in solution.

Conclusion

MPDP Compound was synthesized and characterized by FT-IR, FT-Raman, UV-Vis, and NMR spectra. The calculated geometrical parameters and harmonic frequencies were in good agreement with

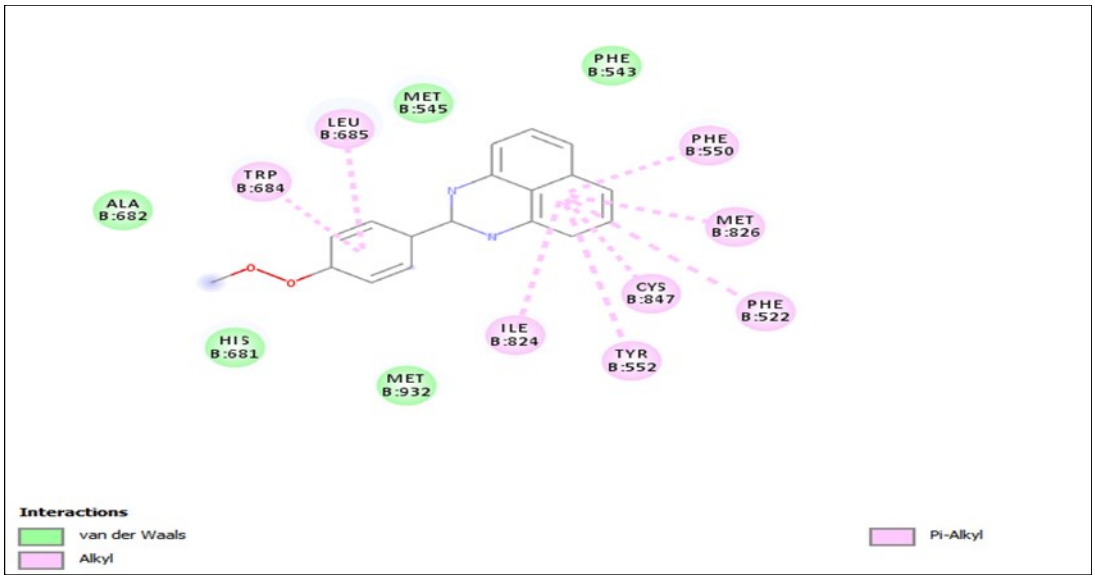

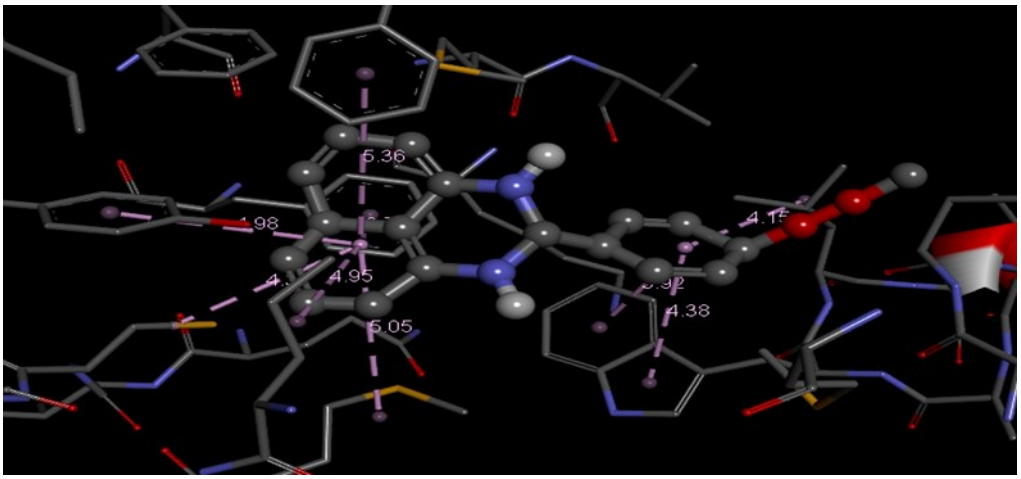

Fig 10. 2d and 3d interaction of compound MPDP

Table 9. Thermodynamic properties at different temperatures of MPDP

T (K)	S (J/mol.K)	Cp (J/mol.K)	ddH (kJ/mol)
100	355.52	110.89	7.13
200	459.34	202.39	22.63
298.15	558.88	303.23	47.43
300	560.76	305.12	47.99
400	662.01	401.14	83.42
500	760.43	481.08	127.67
600	854.01	544.97	179.1
700	942	596.07	236.24
800	1024.39	637.57	297.99
900	1101.53	671.79	363.52
1000	1173.83	700.37	432.17

literature values. A complete vibrational analysis was made for the first time to the molecule MPDP. The N17-C21-N18 ring portion attained twisted boat configuration due to steric effect. The first order hyperpolarizability (β0) value is eighteen times greater than that of urea and hence the present molecule possesses good NLO property. The LP O33 atom transfer more energy: 77.86 kj/mol to anti-bonding orbital π* (C26-C30), which may be due to the involvement of lone pair electrons in oxygen of methoxy group in energy state. The calculated band gap energy was 4.057ev. The calculated UV-Vis spectral values are in good agreement with the observed values. The absorption maximum 276 was assigned to π-π* type. The MEP surface plot represents the reactive sites of nucleophilic and electrophilic attack. The thermodynamic parameters (entropy, enthalpy and heat capacity) are calculated in the temperature range from 100 to 1000k. In addition Mulliken atomic charges and various physico-chemical properties are also calculated. The docking study indicate that the molecule MPDP possessis high binding energy -13.23kcal/mol, which may be due to the Vander walls and π-alkyl interactions.

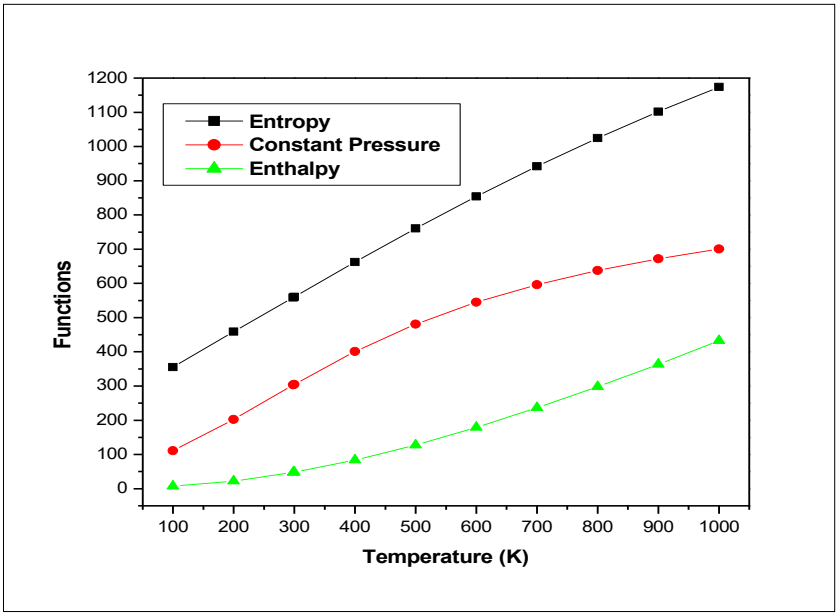

Fig 11. Correlation graphs between thermodynamic functions VS temperatures of MPDP

References:

1. Casas, J. S., Castellano, E. E., Couce, M. D., Ellena, J., Sánchez, A., Sordo, J., Taboada, C. (2006) A gold(I) complex with a vitamin K3 derivative: Characterization and antitumoral activity, J. Ing. Bio.Chem., 100: 1858–1860.
2. West, D. X., Liberta, A. E., Padhye, S. B., Chikate, R. C., Sonawane, P. B., Kumbhar, A. S., Yerande, R. G. (1993) Thiosemicarbazone complexes of copper(II): structural and biological studies, Coord. Chem. Reviews, 123: 49–71.
3. Rodriguez-Argüelles, M. C., Ferrari, M. B., Fava, C. Pelizzi, G. G., Tarasconi, P., Albertini, R., Dall'Aglio, P. P., Lunghi, P., Pinelli , S. (1995) 2,6-Diacetylpyridine bis (thiosemicarbazones) zinc complexes: Synthesis, structure, and biological activity, J. Inorg. Biochem, 58: 157–175.
4. Casas, J., García-Tasende, M. S., Maichle-Mössmer, C., Rodríguez-Argüelles, M. C., Sánchez, A., Sordo, J., Vázquez-López, A., Pinelli, S., Lunghi, P., Albertini, R. (1996) synthesis, structure, and spectroscopic properties of acetato (dimethyl) (pyridine-2-carbaldehydethiosemicarbazonato)tin(IV) acetic acid solvate, [SnMe2 (PyTSC)(OAc)].HOAc. Comparison of its biological activity with that of some structurally related diorganotin (IV) bis (thiosemicarbazonates), J. Inorg. Biochem. 62-41–55.
5. Ferrari, M. B., Fava, G. G., Tarasconi, P., Albertini, R., Pinelli, S., Starcich, R. (1994) Synthesis, spectroscopic and structural characterization, and biological activity of aquachloro (pyridoxal thiosemicarbazone) copper(II) chloride, J. Inorg. Biochem. 53- 13–25.
6. Koch, U., Attenni, B., Malancona, S., Colarusso, S., Conte, I., Di Filippo, M., Harper, S., Pacini, B., Giomini, C., Thomas, S., Incitti, I., Tomei, L., De Francesco, R., Altamura, S., Matassa, V. G., Narjes,

F. (2006) 2-(2-Thienyl)-5,6-dihydroxy-4-carboxypyrimidines as Inhibitors of the Hepatitis C Virus NS5B Polymerase: Discovery, SAR, Modeling, and Mutagenesis, J. Med. Chem. 49-1693–1705.

7. Zamora, F., Kunsman, M., Sabat, M., Lippert, B. (1997). Metal-Stabilized Rare Tautomers of Nucleobases. 6. † Imino Tautomer of Adenine in a Mixed-Nucleobase Complex of Mercury (II) , Inorg. Chem., 36: 1583–1587.
8. Jolibois, F., Cadet, J., Grand, A., Subra, R., Rega, N., Barone, V. (1998) Structures and Spectroscopic Characteristics of 5,6-Dihydro-6-thymyl and 5,6-Dihydro-5-thymyl Radicals by an Integrated Quantum Mechanical Approach Including Electronic, Vibrational, and Solvent Effects, J. Amer. Chem. Soc. 120: 1864–1871.
9. Katritzky, A.R., Pees, C.W., Boulton, A.J. , Mckillop, C. J. (1984) Heterocycl, Chem. 3: 57.
10. Pokladko, M., Gondek, E., Sanetra, J., Nizioł, J., Danel, A., Kityk, I. V., Reshak, A. H. (2009) Spectral emission properties of 4-aryloxy-3-methyl-1 -phenyl-1H-pyrazolo [3, 4-b] quinolines, Spectro-chim. Acta Part A: Molecular and Bio. Spectro. 73: 281–285.
11. Fuks-Janczarek, I., Reshak, A. H., Kuźnik, W., Kityk, I. V., Gabański, R., Łapkowski, M. Motyka, R., Suwiński, J. (2009) UV–vis absorption spectra of 1,,-dialkoxy-2,5-bis[2-(thien-2-yl)ethenyl]benzenes, Spectrochim. Acta Part A: Mol. Biomol. Spectros. 72: 394–398.
12. Reshak, A. H., Stys, D., Auluck, S., Kityk, I. V. (2010) Linear and Nonlinear Optical Susceptibilities of 3-Phenylamino-4-phenyl-1, 2, 4-triazole-5-thione, J. Phys. Chem. 114: 1815–1821.
13. Reshak, A. H., Auluck, S., Stys, D., Kityk, I. V., H. Kamarudin, J. Berdowski, and Z. Tylczynski (2011) Dispersion of linear and non-linear optical suscepti-bilities for amino acid 2-aminopropanoic CH3CH (NH2)COOH single crystals: experimental and theoretical investigations," J. Mater. Chem. 21: 17219.
14. Reshak, A. H., Kamarudin, H., Auluck, S. (2012) Acentric Nonlinear Optical 2,4-Dihydroxyl Hydrazone Isomorphic Crystals with Large Linear, Nonlinear Optical Susceptibilities and Hyperpolarizability, J. Phys. Chem. 116: 4677–4683.
15. Reshak, A. H., Kamarudin, H., Auluck, S. (2013) Electronic structure, density of electronic states, and the chemical bonding properties of 2,4-dihydroxyl hydrazone crystals (C13H11N3O4), J. Mater. Sci. 48: 3805–3811.
16. Reshak, A. H., Kamarudin, H., Kityk, I. V., Auluck, S. (2013) Electronic structure, charge density, and chemical bonding properties of C11H8N2O o-methoxydicyanovinylbenzene (DIVA) single crystal, J.ournal of Materials Science, 48: 5157–5162.
17. Chernyshev, V. M., Pyatakov, D. A., Sokolov, A. N., Astakhov,3 A. V., Gladkov, E. S., Shishkina, S. V., Shishkin, O. (2014) Partially hydrogenated 2-amino [1,2,4]triazolo[1,5-a]pyrimidines a synthons for the preparation of polycondensed heterocycles: reaction with chlorocarboxylic acid chlorides, Tetrahedron. 70: 684-701.
18. Kanbara, T., Kushida, T., Saito, N., Kuwajima, I. Kubota, K., Yamamoto, T. (1992) Preparation and Properties of Highly Electron-accepting Poly (pyrimidine-2,5-diyl," Chem. Lett. 21: 583–586.
19. Meyer, T. J. (1989) Chemical approaches to artificial photosynthesis," Acc. Chem. Res 22: 163–170, May.
20. Pavluchenko, A. I., Petrov, V. F., Smirnova, N. I. (1995) Liquid crystalline 2,5-disubstituted pyridine derivatives," Liquid Crystals. 19: 811–821.
21. Beena, K. P., Akelesh, T. (2012). Int. Res. J. Pharm. 3: 303–304.
22. Asghari, S., Tajbakhsh, M., Kenari, B. J., Khaksar, S. (2011) Supramolecular synthesis of 3, 4-dihydropyrimidine-2(1H)-one/thiones under neat conditions, Chinese Chem. Lett. 22: 127–130.
23. Alam, M., Lee, D.U. (2016) synthesis, spectroscopic and computational studies of 2-thiophen-2yl)-2, 3-

dihydro-1H-Perimidine: An enzymes inhibition study," computational biology and chemistry 64: 185 -201.

24. Wasulko, W., Noble, A.C., Popp, F.D. (1966) Synthesis of potential antineoplastic agents XIV. Some 2-substituted 2, 3-dihydro-1H-perimidines, J. Med. Chem. 9: 599–601.
25. Frisch, M.J. (2004) Gaussian 03, Revision C.02, Gaussian Inc," Wallingford, CT.
26. Schlegel, H.B. (1982) Optimization of equilibrium geometries and transition structures," J. Com. Chem.3: 214–218.
27. Jamroz, M.H. (2004) Vibrational Energy Distribution Analysis: VEDA4 program," Warsaw, Poland.
28. Frisch, A. (2000) Nielson, A.B., Holder, A.J. Gauss view user manual," Gaussian Inc, Pittsburgh PA.
29. Michalska, D. (2003) Raint Program," Wroclaw University of Technology.
30. Michalska, D., Wysokinski, R. (2005) The prediction of Raman spectra of platinum (II) anticancer drugs by density functional theory," Chem. Phys. Lett. 403: 211–217.
31. Jamroz, M.H. (2004) Vibrational Energy Distribution Analysis: VEDA4 program," Warsaw, Poland.
32. Rauhut, G., Pulay, P. (1995) transferable Scaling Factors for Density Functional Derived Vibrational Force Fields," J. Phys. Chem. 99: 3093-3100.
33. 33. Li, Z., Deng, W. (2011) Synthesis, characterization, crystal structure and DFT studies on 1′, 3′-dihydrospiro [fluorene-9, 2′-perimidine," Spectrochim. Acta Part A: Mol. Biomol. Spectros. 82: 56-62.
34. Socrates, G. (1980) Infrared characteristic group Frequencies 3rd Ed., Wiley Interscience," Pubs., New York.
35. Socrates, G. (2001) Infrared and Raman characteristic group frequencies-Tables and charts 3rd Ed., Wiley: New York.
36. Meganathan, C., Sebastian, S., Kurt, M., Woo Lee, K., Sundaraganesan, N. (2010) Molecular structure, spectroscopic (FTIR, FTIR gas phase, FT-Raman) first-order hyperpolarizability and HOMO-LUMO analysis of 4-methoxy-2-methyl benzoic acid," J. Raman Spectrosc. 41: 1369–1378.
37. Lakshmaiah, B., Ramana Rao, G. (1989) Vibrational analysis of substituted anisoles. I-Vibrational spectra and normal coordinate analysis of some fluoro and chloro compounds," J. Raman Spectrosc. 20: 439-448.
38. Lakshmaiah, B., Ramana Rao, G. (1991) Indian J. Pure Appl. Phys. 29:370.
39. Venkataram Reddy, B., Ramana Rao, G. (1994) Transferable valence force fields for substituted benzenes," Vibrational Spectrosc. 6: 231-250.
40. Ashok Babu, V., Lakshmaiah, B., Sree Ramulu, K., Ramana Rao, G. (1987) Indian J. Pure Appl. Phys. 25: 58.
41. Silverstein, M., Basseler, C.G., Morill, C. (1981) Spectrometric Identification of Organic Compounds, Wiley, New York.
42. Khalaji, A. D., Chermahini, A. N., Fejfarova, K. Dusek, M. Synthesis, characterization, crystal structure, and theoretical studies on Schiff-base compound 6-[(5-Bromopyridin-2-yl) iminomethyl] phenol, Struct. Chem. 21:153-157.
43. Varghese, H.T., Panicker, C.Y., Madhavan, V.S., Mathew, S., Vinsova, J. (2009) FT-IR, FT-Raman and DFT calculations of the salicylanilide derivate 4-chloro-2-(4-bromophenylcarbamoyl phenyl acetate," J. Raman Spectrosc. 40: 1211–1223.
44. Varsanyi, G. (1974) Assignments of vibrational spectra of 700 Benzene Derivatives, Wiley, New York.
45. Coe, B.J., Harris, J.A., Jones, L.A., Brunschwig, B.S., Song, K., Clays, K., Garın, J., Orduna, J., Coles, S.J., Hursthouse, M.B. (2005) Syntheses and Properties of Two-Dimensional Charged Nonlinear Optical Chromophores Incorporating Redox-Switchable cis -Tetraammineruthenium(II) Centers . J. Ameri. Chem. Society.127:4845–4859.
46. Reed, A.E., Weinhold, F. (1985) Natural localized

molecular orbitals, J. Chem. Phy.83: 1736–1740.

47. Reed, A.E., Weinstock, R.B., Weinhold, F. (1985) Natural population analysisa. J. Chem. Phy. 83:735–746.
48. Reed, A.E., Weinhold, F. (1983) Natural bond orbital analysis of near-Hartree–Fock water dimer," J. Chem. Phy. 78: 4066–4073.
49. Foster, J.P., Wienhold, F. (1980) Natural hybrid orbitals. J. Ameri. Chem. Society. 102:7211–7218.
50. Chocholousova, J., Vladimir Spirko, V., Hobza, P. (2004) First local minimum of the formic acid dimer exhibits simultaneously red-shifted O–H□O and improper blue-shifted C–H□O hydrogen bonds," Journal of Chemical Physics. 6: 37–41.
51. Fleming, I. (1976) Frontier Orbitals and Organic Chemical Reactions, Wiley, London.
52. Gunasekaran, S., Kumaresan, S., Arunbalaji, R., Anand, G., Srinivasan, S. (2008) Density functional theory study of vibrational spectra, and assignment of fundamental modes of dacarbazine," J. Chem. Scien. 120: 315-324.
53. Bevan Ott, J., Boerio-Goates, J. (2000) Introduction," Chemical Thermodynamics: Principles and Applications, Academic Press, San Diego.